BEng Aeronautical Engineering

Academic Year 2021-2022

ET3107: Project Dissertation

Project Title: *Design of a Turboexpander for Energy Recovery from a Gas let-down station for Blended Natural Gas and Hydrogen Grid*

Student Name: *Abdul-Rahman Asankomah*

Supervisor Name: Dr. Jafar Al-Zaili

Acknowledgements

TBC

Nomenclature & Acronyms

A	Area [m^2]
D	Diameter [m]
V	Velocity [m/s]
Cp	Specific heat at constant pressure [KJ/Kg K]
ρ	Density [kg/m^3]
U	Blade Speed [m/s]
N	Rotational Speed of Impeller [rpm]
w	Relative fluid velocity [m/s]
c	Absolute fluid velocity [m/s]
h	Specific Enthalpy [KJ/kg]
W	Specific work [KJ/kg]
Q	Heat transfer [KJ/kg]
Re	Reynolds Number
T	Temperature [K]
η_{T-T}	Total-Total Efficiency
η_{T-s}	Total-to Static Efficiency
$\dot{m}$	Mass flow rate [kg/s]
E	Energy [KJ]
r	Radius [m]
s	Entropy [KJ/Kg K]
Ω_s	Specific speed [rad]
N_s	Dimensionless specific speed
P	Pressure [Pa]
IFR	Inward-Flow Radial
PRS/GRS	Pressure/ Gas Regulation Station
δ	Boundary Layer thickness

Subscripts

0	Total Property at stagnation
1-4	Turbine state points
r	Rotor
rel	Relative
t-t	Total-to-total
t-s	Total-to-static
s	Isentropic

List of Figures

List of Tables

1. Abstract

TBC

Keywords: Radial Turbine, Hydrogen, BladeGen

2. Introduction

With the advent of COP26, there has not been a more important time than now to adopt efficient ways of producing energy and reducing harmful emissions. The gas grid is an important and highly integrated infrastructure for the transport of natural gas through countries around the world. The network consists of gathering systems, gas processing plants, wide diameter transmission pipelines and small diameter low pressure service lines. In 2020 alone, the natural gas transportation network in the U.K delivered over 27.7 trillion cubic feet of natural gas to almost 21 million homes. Unfortunately, the process through which the pressure of the gas is lowered before distribution is energy inefficient as the kinetic energy of the working fluid is not made well use of. Loses of up to 7.5MW have been recorded at some stations. In place of a pressure valve, turboexpanders are proposed as a means to recover some of the pressure energy, which can then be used to generate electricity. Hydrogen can be injected into the grid as a method to reduce the combustion of methane. Due to end-user systems constraints, the existing turbomachine blade designs cannot accommodate for a blended network. Thus, this project will focus on generating blade designs for different blend ratios and make a recommendation on the design that is most efficient. To capture the blade design requirements, the operating thermodynamic conditions of a typical gas let-down station will be utilized. The GRS operating conditions will also allow investigation into how the design will work under real conditions. CFD is a powerful tool that will be utilized to assess how the turbine would operate in different gas blend cases involving hydrogen and natural gas.

3.Background

A gas grid is an integrated network of objects and systems to transport and distribute natural gas. The components include underground natural gas storages, compressor stations, Gas Regulation Stations (GRS), and gas pipelines (Szoplik, 2012). The gas compression process is required as the gas loses pressure after traveling for long distances in the pipes. The component of interest in this project is the GRS, of which several types can be considered. GRS stations are characterised by various parameters and can broadly be divided into high-pressure reduction, middle-pressure reduction, metering, and distribution stations. Szoplik (2012) highlights the pressure characteristics of each gas pipeline system, and figure 3. 1 shows a schematic of a typical layout of a natural gas distribution network. Middle pressure reduction stations supply natural gas in the order of $\sim 1\ MPa$ for industrial and commercial uses, which are essential to the economy. Consequently, the turbomachinery design will be made to operate at these types of stations.

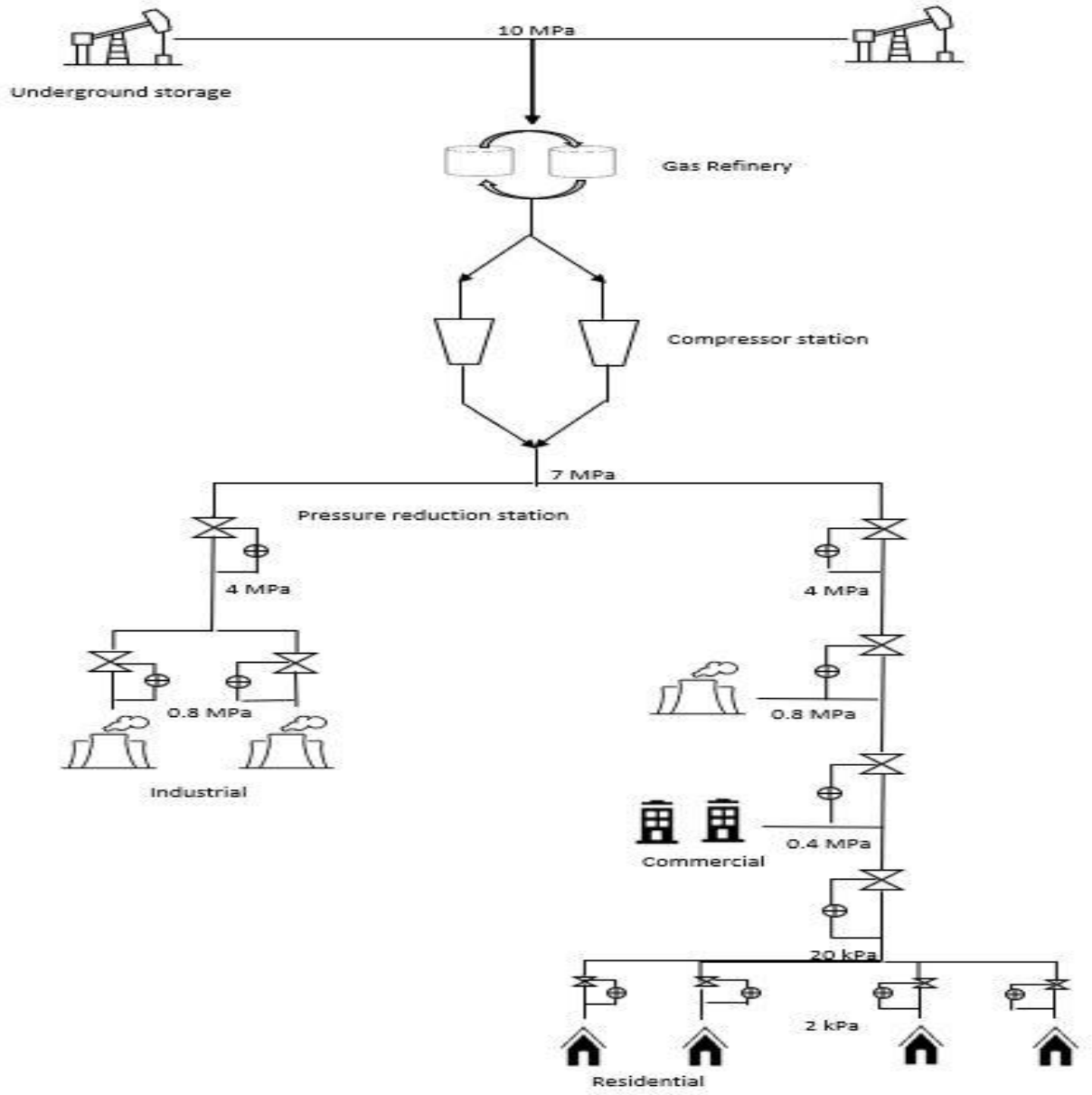

Figure 3. 1 A typical Natural Gas Distribution Network (made via Microsoft Visio and Word)

The use of valves such as Joule-Thompson valves for pressure reduction still dominates in most pressure-reducing stations. This method of pressure regulation is inefficient as it involves energy dissipation that results in irreversible losses in the gas stream (Kuczynski et al., 2019a). Moreover, electricity consumption increased by 743% between the early 80s and 2010 (Neseli, Ozgener, and Ozgener, 2015). Thus research based on boosting productivity in energy production can play a critical role in energy recovery. From this standpoint, this project is of great importance.

Over 180 years ago, the radial flow turbine, the outflow type, was first conceived for hydraulic power generation. A much highly regarded turbine, mainly due to the thermodynamic benefits associated with the flow path is the radial-inflow type, which was developed in 1847 by Francis and Boyden in the USA. The inward-flow radial (IFR) turbine is flexible due to the ranges of power it can cover, mass flow rates

and rotational speeds. This makes them an excellent choice to use in turbomachines at gas let-down stations as they could extract more work from the working fluids and are generally easier to manufacture, making them scalable.

Of the two main types of IFR turbines namely the 90º IFR and cantilever turbine, the latter requires an increase inflow area resulting from the rotor expansion, which is difficult to accommodate for(Dixon & Hall, 2010). The 90 degrees IFR has a greater structural strength compared to the cantilever entailing that the rotor vanes can accommodate for high stress levels induced by centrifugal forces. Thus, they would be the focus of this design enterprise.

3.1 Zero-dimensional Analysis: Thermodynamics of a 90° IFR Turbine

The properties of interest that defines the thermodynamic state of an ideal fluid include pressure and temperature as well as velocity and flow angles. Figure 3.1.1 shows a typical layout and associated velocity diagrams of a 90-degree IFR turbine. The stations are explained as follows:1 – nozzle inlet, 2 – nozzle exit/ rotor inlet, 3 – rotor exit / diffuser inlet, 4 – diffuser exit.

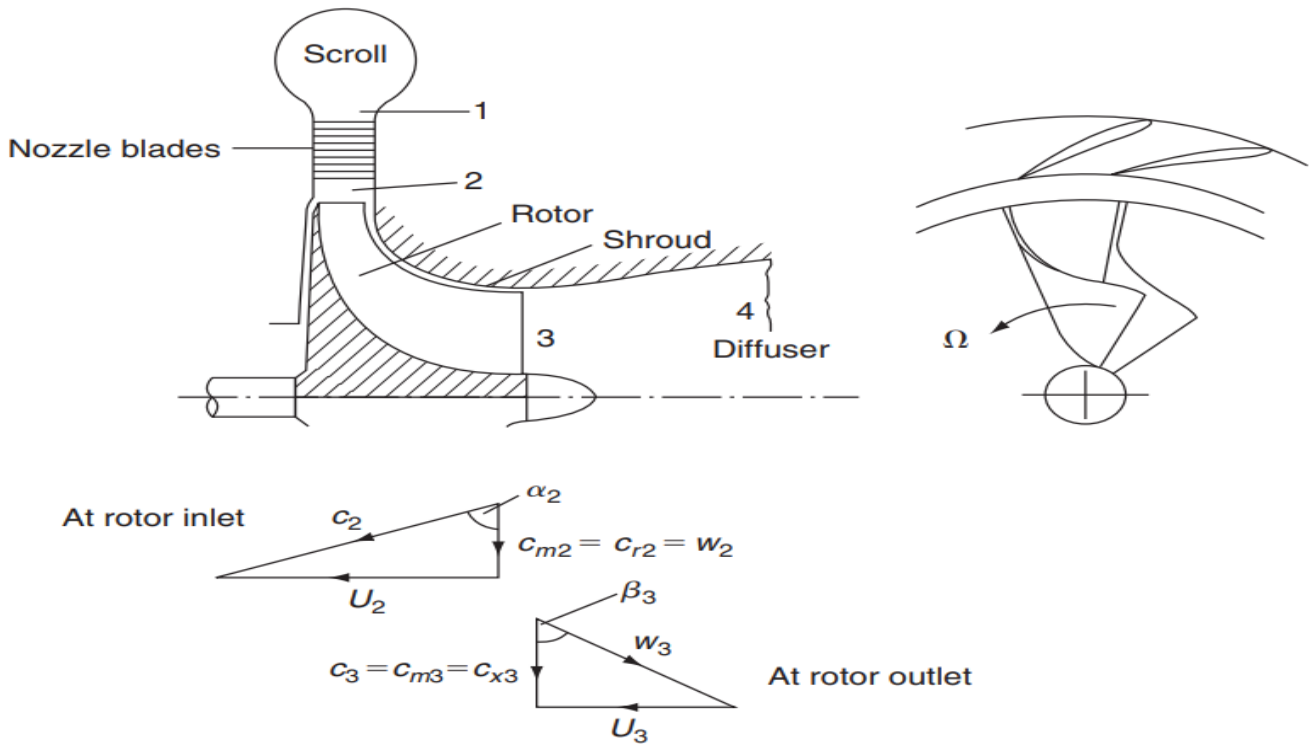

Figure 3. 2 Layout and Velocity Diagram representing the nominal design condition for a 90-degree IFR Turbine

The fluid enters at station 1 with an absolute velocity c1 (not shown),where it is accelerated by the nozzle to a higher absolute velocity of c2. The flow moves into station two with a radial velocity of w2, which is at angle of α2 to c2. The rotational speed of the rotor is Ω and U_2 is its tangential tip velocity. At this section (station two), the rotor vanes extend radially inward and turn the flow through a 90-degree turn, a velocity decreasing process. At station 3, the gas exits the turbine axially with an absolute speed of C3 and enters the diffuser with a flow angle of β3 and a radial velocity, w3. The tangential speed of the rotor is different and is equal to U3.The flow eventually exists the diffuser at station four.

For all intents and purposes, the flow will also be considered steady, thus the continuity equation can be invoked to develop a relationship between rotor inlet and outlet conditions:

$$\dot{m} = \rho_2 * w_2 * A_2 = \rho_3 * w_3 * A_3 = constant \ldots (1)$$

From an energy balance of a system (first law of thermodynamics), the net change in the total energy during a process is equal to the total energy entering the system and the total energy leaving that system (Cengel, Boles, kanoglu,2018):

$$E_{in} - E_{out} = \Delta E_{system} \ldots (2)$$

Equation 2 gives rise to steady flow energy equation (Equation 3), which needs to be considered as a logical design starting point since a rotor is essentially a work transfer device (Whitfield and Banes, 2010).

$$\frac{\dot{Q}}{\dot{m}} - \frac{\dot{W}}{\dot{m}} = (h_2 - h_1) + \frac{1}{2}(C_2^2 - C_1^2) + g(z_2 - z_1) \ldots (3)$$

For the turbomachines being considered, the potential energy term is negligible.

Applying the adiabatic condition to Equation 3 and making the appropriate sign changes for a turbine (since heat in or work-in is zero) yields:

$$\frac{\dot{W}}{\dot{m}} = \left(h_1 + \frac{1}{2} C_1^2\right) - \left(h_2 + \frac{1}{2} C_2^2\right) = (ho_{in} - ho_{out}) = C_p(toin - tout) \ldots (4)$$

Furthermore, the specific work on the rotor by the fluid is given by the Euler turbomachinery equation below (Equation 5) and can be manipulated using the velocity triangles to define the work transfer per unit mass from station one to three in terms of rotor and fluid velocities (Equation 6):

$$\Delta W = h_{01} - h_{03} = U_2 C_{\theta 2} - U_3 C_{\theta 3} \ldots (5)$$

Since the stagnation enthalpy across the nozzle is constant $h_{01} = h_{02}$, Equation 5 manipulated to obtain Equation 6:

$$\Delta W = h_{02} - h_{03} = \frac{1}{2}[(U_2^2 - U_3^2) - (w_2^2 - w_3^2) + (C_2^2 - C_3^2)] \ldots (6)$$

All three terms in Equation 6 contribute to the specific work output. Since the first term is positive for a turbine as $U_2 > U_3$, it translates into a greater energy extraction from the fluid turbine compared to axial turbine where $U_2 = U_3$.

The Mollier diagram, Figure 3.3, illustrates the expansion process for the IFR turbine layout shown in Figure 1. The expansion process is ideally one that is irreversible and adiabatic between stations 2 and 3, from the second law of thermodynamics. However, there is an increase in entropy from station two to three as indicated by Equation (7):

$$s_3 > s_2 \ldots (7)$$

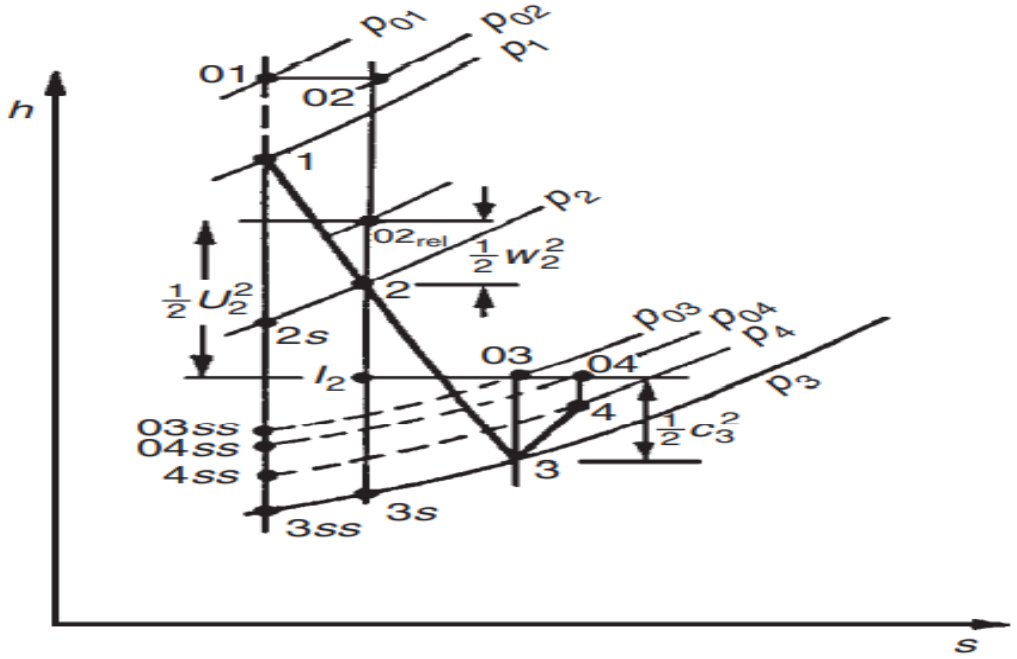

Figure 3. 3 Mollier Diagram for 90- degree IFR Turbine

The work output can be made a simple function of blade speed only (Equation 8) by setting the flow angle at the inlet relative to the blade equal to zero and assuming that the exit velocity is axial from Equation 5.

$$\Delta W = U_2^2 \ldots (8)$$

One of the most important parameters of turbomachinery design is the efficiency. For an expander, this is generally defined as:

$$\eta_T = \frac{Actual\ work\ output}{Work\ output\ in\ an\ ideal\ process\ between\ two\ defined\ end\ states} \ldots (9)$$

The efficiency will be defined using station one, which is the stagnation state (since this is where the fluid has maximum kinetic energy) and station 3 as the outlet. The ideal process of interest will be isentropic as the expansion process is considered adiabatic. Within this definition, This efficiency will only consider blade losses and exit kinetic energy internal losses of the fluid. Thus, for a turbine operating on an ideal gas and for $T_1 > T_2$:

$$\eta_{Ts} = \frac{h_{01} - h_{03}}{h_{01} - h_{3s}} \ldots (10)$$

$$\eta_{Ts} = \frac{W_{actual}}{W_{ideal}} = \frac{\dot{m}C_p(T_1 - T_2)}{\dot{m}C_p(T_1 - T_2')} = \frac{T_1 - T_2}{T_1 - T_2'} \quad (11)$$

In turbomachinery design, there are two main types of efficiency to investigate: the total-total and total-

to-static efficienies, of which the latter is greater than the former. The isentropic efficiency is given by Equation (11) is of prime importance in this investigation as the flow at the exit should have some kinetic energy, which should be as low as possible without reaching zero. A typical value for an IFR turbine operating at a gas letdown station is about $\eta_{Ts} = 80 - 85\%$. An efficney of 80% will be used as a starting approximation and the actual value will later on be confirmed. Rohlik (1990) discovered that there a limited range of specificif speed, N_s, that can a produce a turbine that has a high isentropic efficney:the value should lie between 0.3 and 0.6 according to Figure 3.4. Since this turbine is to be designed for the highes efficiency, a corresponding value of 0.3 would be used and later verfied in Vista RTD.

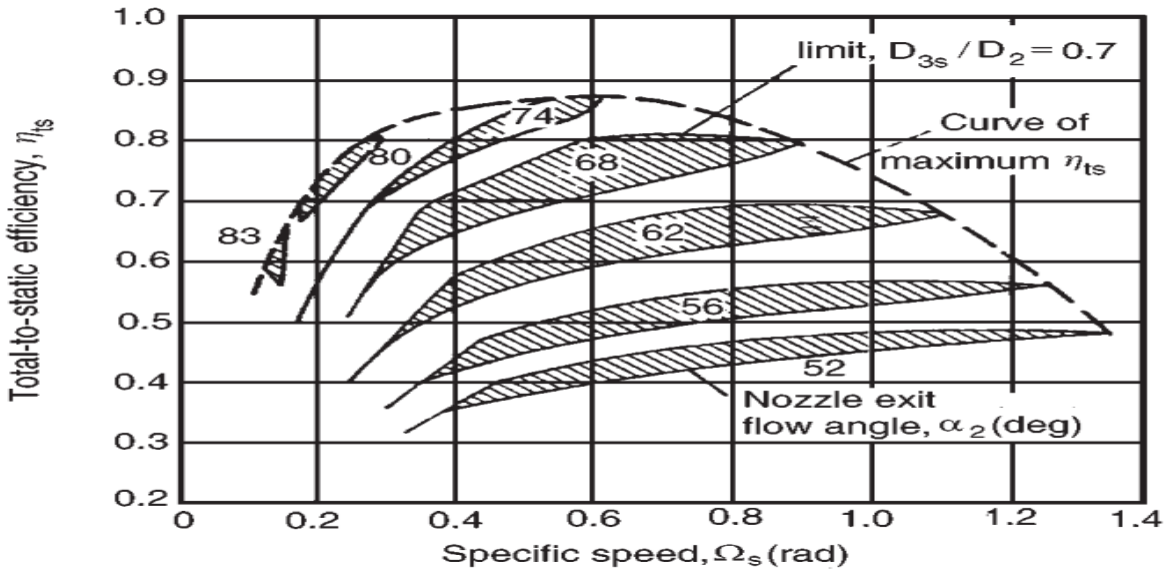

Figure 3. 4 Rohlik 1990, 90 degrees IFR turbine performance

In an early study of IFR turbine design for maximum efficiency, Rohlik (1968) specified that the ratio of the rotor shroud diameter to rotor inlet diameter should be limited to a maximum value of 0.7 to avoid excessive shroud curvature and that the exit hub–shroud tip ratio was limited to a minimum of 0.4 to avoid excess hub blade blockage and loss. At the best efficiency point of actual (frictional) 90° IFR turbines it is found that this velocity ratio is, generally, in the range 0.68 < U2/c0 < 0.71.

3.2 Energy analysis

The use of an expansion turbine requires an energy analysis for many reasons. For instance, the gas temperature must remain above the hydrate zone and dew point (255K) to prevent the pipes from becoming brittle, whocih could lead to structural failures.Two methods of overcoming this problem is to either use some of the recovered energy to pre-heat the gas (before it enters the turbine inlet) or post-heat the gas at the exit so that it is close to the inlete temperature. The energy efficient process will be proposed following the analysis. For both cases, the temperature of the gas entering the GRS is 300K and the temperature of the gas leaving the GRS is 290K and there are some variables that must remain fixed: η_{Ts}, P_r, and $\dot{m}$.

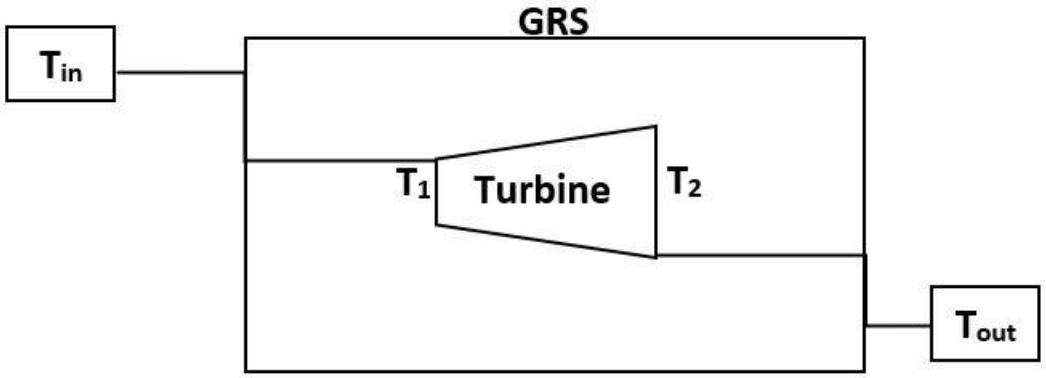

Figure 3. 5: Rudimentary sketch showing the temperature in the gas pipelines that enter & leave the station, T_{in} and T_{out} as well as the temperature that leaves and enters the turbine, T_1 & T_2.

From Figure 3.5, an isentropic expansion can be considerd, which leads to the following equation:

$$\left(\frac{T_2'}{T_1}\right) = \left(\frac{P_2}{P_1}\right)^{\frac{\Upsilon-1}{\Upsilon}} \quad (12)$$

The heat energy required to heat the fliud is given by:

$$\dot{q} = \dot{m}\overline{C_p}\Delta \quad (13)$$

The variable $\overline{C_p}$ is an average value obtained by finding the average temperature and subsitutung it into the the polynomial function of C_p, which is shown in the Appendix.

In the case of preheating, T2 is fixed,where $T_2 \approx T_{out} \cong 290K$. T_2' and T_1 are unknown, however Equation (11) and (12) can be manipulated to determine the value of T_1 by forming a relation between T_1 and T_2'. For post-heating, T_1 is fixed and $T_1 \approx T_{in} \cong 300K$. After deteriming the heat required to heat the fluid, the power of the turbine and net power could be calculated using Equation (14) and (15) respectively. The specfici power was also obtained from Equation (16). The computation was completed using MATLAB and the results are summarised in Table 3.1 for both cases.

Table 3. 1: Summary of Energy Analysis

Option	*T1/K*	*T2/K*	*$\dot{q}$/kW*	*$\dot{W}_T$/kW*	*$\dot{W_{net}}$/kW*	*ΔW/ KJ/kg*
Preheat	*355.9*	*290*	*1438*	*1696*	*124*	*11.15*
Post-heat	*300*	*236.3*	*1259*	*1494*	*117*	*10.53*

Power from turbine is:

$$\dot{W}_T = \dot{m}\overline{C_p}(T_1 - T_2) \quad (14)$$

The net power is given by:

$$\dot{W_{net}} = \eta_{mechanical} * W_T * \eta_p - \dot{q} \quad (15)$$

The spefic power is given by:

$$\Delta W = \frac{\dot{W}}{\dot{m}} \quad (16)$$

From Table 3.1, a net electrical enegery output is possible in both options and this is better than using an expansion valve as you can get some postive net output. From this analysis, it is much more efficienct to post-heat the working fliud as an extra 5.5% of energy can be extracted from the process leading to a more efficient GRS.As the temperature of 236.3K at the turbine exit is 7% below 255K, the pipes in this vicinity can be constructed from a different material compared to the rest of the pipe in the network. For instance stainless steel can still maintain its mechanical integrity at low temperatures of $-40℃$. The heating process can also begin immediately after the duct of the turbine so shorten the length of pipe that needs this modifcation.

4.Literature Review

4.1 The utilisation of Turbo-expanders in Existing GRS

Turboexpanders are rotating devices that convert the pressure energy of gases into mechanical work. From several case studies observed, GRS stations that are eligible to have a turboexpander installed have reaped the benefits in the form of gas pressure reductions and energy recovery. Neseli, Ozgener, and Ozgener, (2015) found that 23% of the energy used in compressor stations were recovered at a gas station in Takestan, Iran. Different types of turbines have been investigated, such as axial impulse turbines (Morgese et al., 2020). The methodology used by Morgese et al., (2020) at a GRS in Austria is innovative and can be extrapolated to the design of radial turbines in this project. A fundamental design process is laid out by (Dixon and Hall, 2010), which goes into the thermodynamic equations used for the main components of the turbine, such as the nozzle, stator, rotor, and diffuser. After defining the turbine design point, the mass flow rate,$\dot{m}$, and boundary conditions such as the inlet and outlet temperatures and pressure can be obtained. The losses in the 90-degree IFR turbine can be analysed to account for irreversibility. The primary geometric parameters and specifications, such as the rotor diameter and inlet and outlet flow angles, can then be estimated from a 1D analysis. An optimisation algorithm in Ansys defines the 2D blade profile, and a 3D CFD simulation is carried out to compute the efficiency. Sam and Ghosh, (2017) utilised Ansys CFX to analyse the flow field of a helium turboexpander, which aided in improving the efficiency of these technologies. Figure 8.12 from Dixon and Hall, (2010) shows that there is a limited range of specific speeds that can produce a high-efficiency turbine. This performance correlation can also be used to check the final design.

The temperature drops per MPa when expansion turbines are used are more significant than traditional pressure regulators (Poživil, 2004). The exit temperature of the turbine must not be too cold to avoid the pipes being brittle and to avoid sulphates from forming. For the exit temperature to be $\sim 300°K$ (ambient temperature) and equal to the inlet temperature, several methods have been proposed. This gas can either be preheated or heated at the exit using
the energy generated from the turbine. The former approach has been explored in great depth. Farzaneh-Gord et al., (2012) examined a solar system method of preheating, which can decrease the capital cost that is usually high at stations where boilers are utilised.
Furthermore, Villecco and Pellegrino, (2010) showed that the device's efficiency could be affected by variabilities and irregularities in boundary conditions. Figure 2 from Kuczynski et al., (2019a) shows a schematic of a gas reducing station where a turboexpander is installed parallel with a traditional reduction station. A similar type of arrangement can also be adopted to account for the variation seen in energy demands as part of this project.

4.2 Turboexpanders for Hydrogen Applications

Currently, 84% of homes in the UK receive their energy supply from a natural gas pipeline network. The UK Climate Change Act 2008 requires the country to decrease 80% GHG emissions by 2050. Several options have been investigated to reach this goal. An important future energy carrier is hydrogen, which is proposed to lower GHG emissions significantly, mainly when produced from low carbon sources (Kuczynski et al., 2019b). Based on the system's existing natural gas characteristics and end-user constraints, an option suggested by Dodds and McDowall (2013) is to inject small amounts of hydrogen into the gas network. Kuczynski et al., (2019b) found that the maximum participation of hydrogen in natural gas should not exceed the range of 15% to 20% by volume. This limit is also consistent with other authors such as Witkowski et al., (2018). Melaina, Antonia and Penev, (2013) also suggested a range of 5% to 15% of hydrogen by volume without increasing associated risks. An analysis using the MARKAL optimisation algorithm suggests that the maximum amount of hydrogen should be introduced by 2035 to reach decarbonization goals by 2050 (Dodds & McDowall, 2013).

In terms of computing blended ideal gas thermodynamic properties, Balmer and Robert T, (2011) demonstrated a straightforward method that can be used. The mass fractions for each blend can be calculated to compute parameters such as the gas constant, which can then be imported to Ansys CFX-pre. For this project, the radial expander will operate at a medium-pressure reduction station in the Czech Republic. Unlike the work done by Požívil, (2004), hydrogen gas will be incorporated into the existing natural gas grid to analyse the effect this has on the performance of the expander. The turbine's size depends on the mass flow rate, which is about 11.13 kg/s at this GRS. The pressure ratio is ~ 3, and N = 40,000rpm.

5.Objectives

This project will explore which method of increasing the outlet temperature is better regarding how much electricity is required, which is critical knowledge that can be addressed. Another area that has not been explored is the impact a $90°$ IFR turbine using a natural gas and hydrogen blend has on the turbine's performance. This project can help deepen the understanding of the performance of a turbine that utilises a blended gas as a working fluid.

5.1 Objective 1: Understand the Design of Radial Turbines

Radial turboexpanders possess their own distinctive characteristics thus an applicable method is needed for their design. The radial turboexpander in this project will be working with compressible gases thus a zero-dimensional analysis will be needed to capture the fluid mechanics and thermodynamic requirements. As with any turbomachine, losses are present and there are design constraints that must not be violated to obtain a useful product at the end of the process. By the end of this objective, a thermodynamic model will be made which contains an initial estimate of the total-static efficiency, η_{ts} of the turbine.

5.2 Objective 2: Identify a suitable Case Study

With clarity on the thermodynamic requirement gained from the first objective, research can be made into existing GRS to characterize the radial expander design. It is important to find a case study where a turboexpander has been used to replace a conventional pressure reduction valve. Parameters of interest at this stage are the pressure ratios, efficiencies, and boundary conditions such as the inlet and outlet pressures and temperatures. By means of a suitable simulation and 3D design software such as Ansys, the thermodynamic model developed from objective 1 will be converted into a 1D model. The 1D model will be used to predict various properties such as the total-static efficiency, the inlet and outlet diameter as well as velocity triangles. A first milestone will be when a natural gas 1D model has

been made and analysed by means of CFD using an appropriate mesh from Ansys TurboGrid. The CFD is a way to evaluate the turboexpander performance, which will be compared against initial estimations.

5.3 Objective 3: Identify Acceptable Gas Blends

After analysing a pure natural gas design, gas blends with hydrogen will be investigated. Due to limitations in the extent of gas blends, the range of blends that will be analysed will not exceed 15% to 20% of hydrogen by volume. Consequently, the number of cases that will be studied will be limited to three. Anything less than three may be insufficient and anything above that may be time-consuming and unnecessary to convey the implications of blended designs. A second milestone will be when all three cases have undergone a CFD analysis with the appropriate meshing.

6. Methodology

Figure 3.1 summarises the proposed methodology in the form of a flowchart. After conducting a literature review and reading various thermodynamics and radial design books, the nominal design point was defined. The governing thermodynamic equation for the rotor is of main concern for this project. The operating conditions such as the mass flow rate, $\dot{m}$, the temperature, T and pressure, P, at the inlet and outlet and rotational speed, N, were defined at this stage. The values were coded in Excel and MATLAB.

The isentropic efficiency is introduced and is coded into Ansys Vista RTD using a trial value to account for losses. After that, the other aerodynamic and geometrical constraints are defined and implemented into the software to obtain the 1D model. The output of this analysis yields the flow angles and total-static efficiency among other parameters. Subsequently, BladeGen can be used to produce the meridional profile and the 3D geometrical model of the blade, which can be transported to TurboGrid for meshing. Finally, the simulation settings and gas parameters can be defined in Ansys CFX-pre followed by a CFD analysis. To reach a satisfactory turbine design, iterations are necessary until convergence is reached. The iteration stops when the efficiency from the CFD analysis is maximised. At the end of this step, the results obtained provides the geometric and aerodynamic parameters to construct the turbine. The hydrogen volume in natural gas blend that will be investigated are: 5%, 10% and 15%. The design process was accomplished based on the predefined parameters such as the total inlet temperature, total inlet pressure, mass flow rate, total to static pressure ratio and rotational speed (rpm).

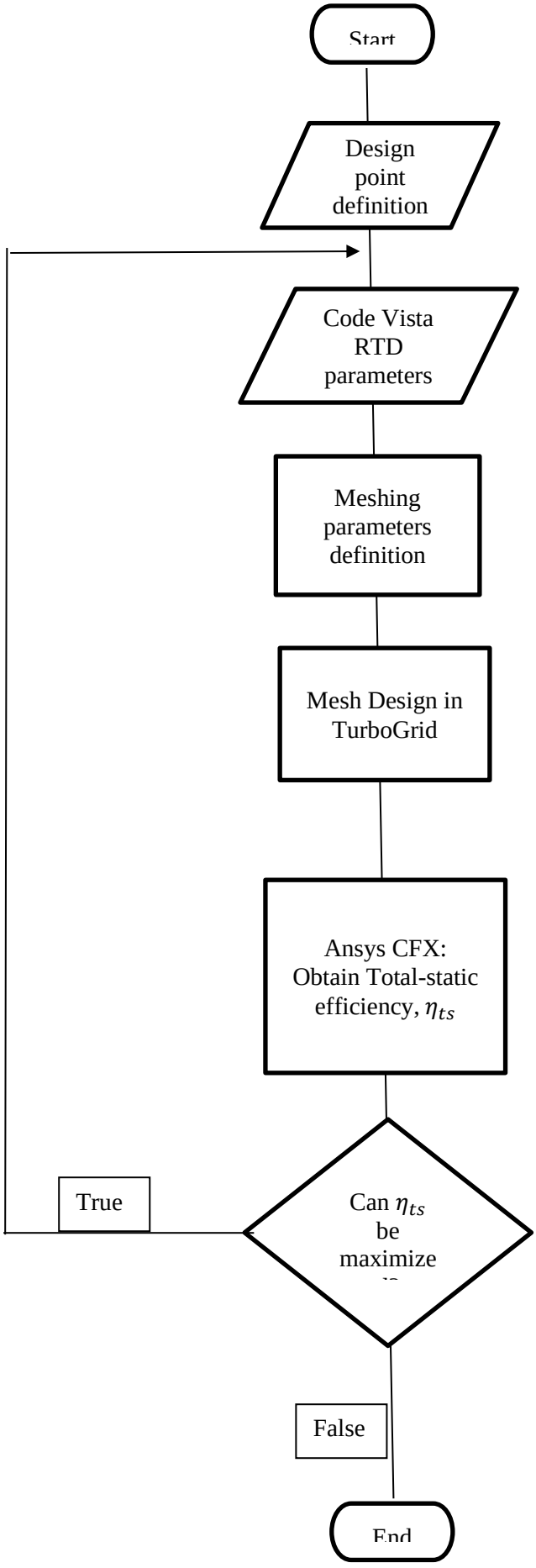
Start
Design point definition
Code Vista RTD parameters
Meshing parameters definition
Mesh Design in TurboGrid
Ansys CFX: Obtain Total-static efficiency, η_{ts}
Can η_{ts} be maximize
True
False
End

6.1 Preliminary design

The turbine operating parameters for natural gas was obtained from a GRS in Velké Němčice, Czech Republic. The 1D model of the blade was designed using the values summarized in Tables 6.1 and 6.2, as part of the preliminary design. Since a one-dimensional flow is of concern in this analysis, it was assumed that the trajectory of the fluid is along streamlines that follow the geometry of the blades. Any slight deviations were considered negligible. Vista RTD is a radial turbine preliminary design tool that allows users to specify aerodynamic and geometric design inputs and returns the blade meridional profile and the results of the analysis. The results of interest include the η_{TS}, N_s, D, inlet and outlet flow angles and the velocity diagrams. Since supersonic conditions should be avoided in the turbine to prevent a decrease in performance, the blades were optimized in an iterative manner to obtain Mach number less than unity, which should be the case for a well-designed rotor. For optimal performance, the exit absolute tangential velocity should be zero, ideally. However, in practical applications, it is reasonable to assume that for a well-designed turbine, the absolute Mach number at the rotor exit has a relatively low value. Thus, efficiency of the turbine was maximized by optimizing the inlet and flow angles such that the relative in-flow angle and the absolute flow angles are close to zero. By doing this, the flow at the rotor inlet can hit the blade at an angle close to 90° absolute angle (ideally) for maximum power extraction and at the exit, the flow could exit parallel to the blade, with an angle of 0° (ideally). The resulting velocity diagrams can be see attached to a blade of radial flow turbine design in figure 6.1.

Table 6. 1: Specified Aerodynamic parameters for Vista RTD

Inlet Stagnation Temperature/ ℃	*Inlet Stagnation Pressure/MPa*	*Mass flow rate/ kg/a*	*Expansion ratio*	*Rotational speed/ rpm*	*Blade speed ratio U/C*	*Total-Total efficiency*	*nozzle efficiency*
300	*5.5*	*11.3*	*3.1*	*40000*	*0.69*	*0.83*	*0.9*

The blade speed ratio (U/c) and total-total efficiency were optimized in such a way to maximize the efficiency of the turbine. The nozzle efficiency was maintained at the default value of 0.9 as it is representative of many radial in-flow turbine designs (Turbosystem user guide).

The number of blades was optimized by utilizing Eqn. (17), the modified Jamieson expression made by Glassman (1976). The initial Jamieson expression shown in Eqn (18) yielded too many blades however Eqn (17) decreases the number of blades required in each design without degrading the performance of the design (reference).

$$n_r = \frac{\pi}{30}(110° - \alpha_2)tan(\alpha_2) \quad (17)$$

For $\alpha_2 = 73°$, $n_r = 13$ blades.

$$n_r = 2\pi tan(\alpha_2) \quad (18)$$

Table 6. 2: Specified Geometric parameters for Vista RTD

Shroud exit/inlet radius	*Hub exit to inlet radius*	*Number of vanes*	*Mean Vane thickness at exit/mm*	*Tip Clearance*
0.7	*0.22*	*13*	*0.991*	*0.01*

6.2 Preliminary design output

The following tables summarize the results obtained from 100% Natural gas turbine completed as part of the preliminary design.

Table 6. 3: Impeller Geometry

Impeller Diameter, mm	Axial length (length/diameter)	Tip clearance/Vane height	shroud clearance	B3 hub	B3 shroud
183.4	0.31	0.01	0.2	52.4	75.9

The axial length of the blade should not be too compared to the diameter of the impeller. The turbine should reduce pressure at the exit however, if the mechanism happens over a short length there will be a lot of losses resulting from flow separation. The flow cannot cope with sudden change in the geometry. Longer blade also means more friction drag due to more surface however it is acceptable compared to the alternative.

Table 6. 4: Inlet and Outlet flow parameters

Inlet flow parameters	Value/deg	Outlet flow parameters	Value/ deg
alpha 2	73	alpha 3	-4
Beta 2	27	Beta 3	-76
M_{abs} inlet	0.81	M_{abs} outlet	0.171

Table 6. 5: Efficiency values and the 1D output specific speed

Parameter	Value
Impeller η_{TT}	84.5
Impeller η_{Ts}	83.2
Stage η_{TT}	83.0
stage η_{Ts}	81.8
Specific speed	0.48

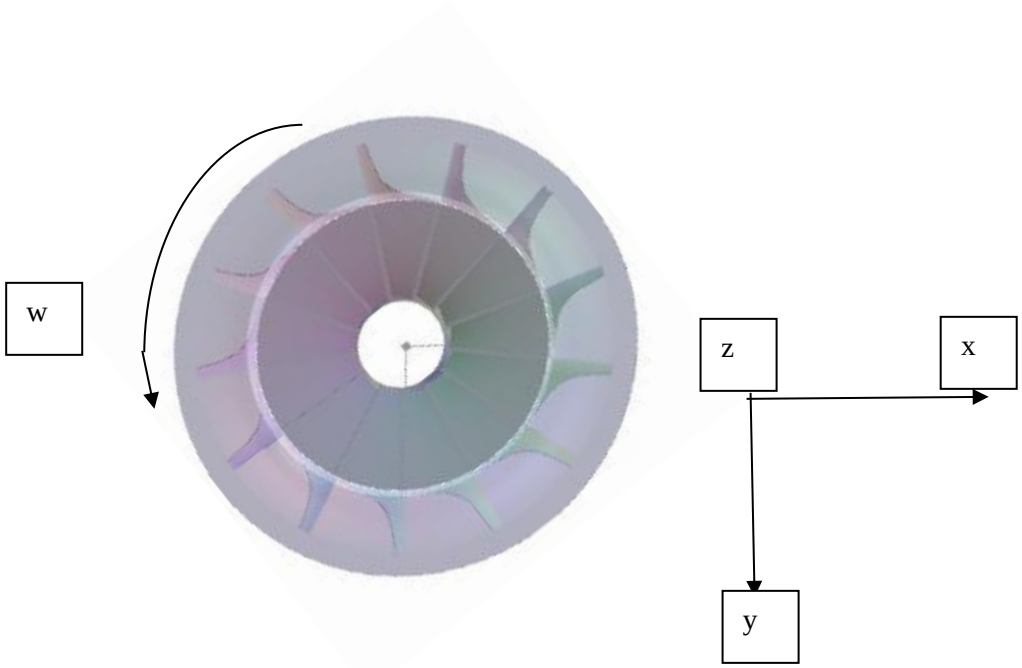

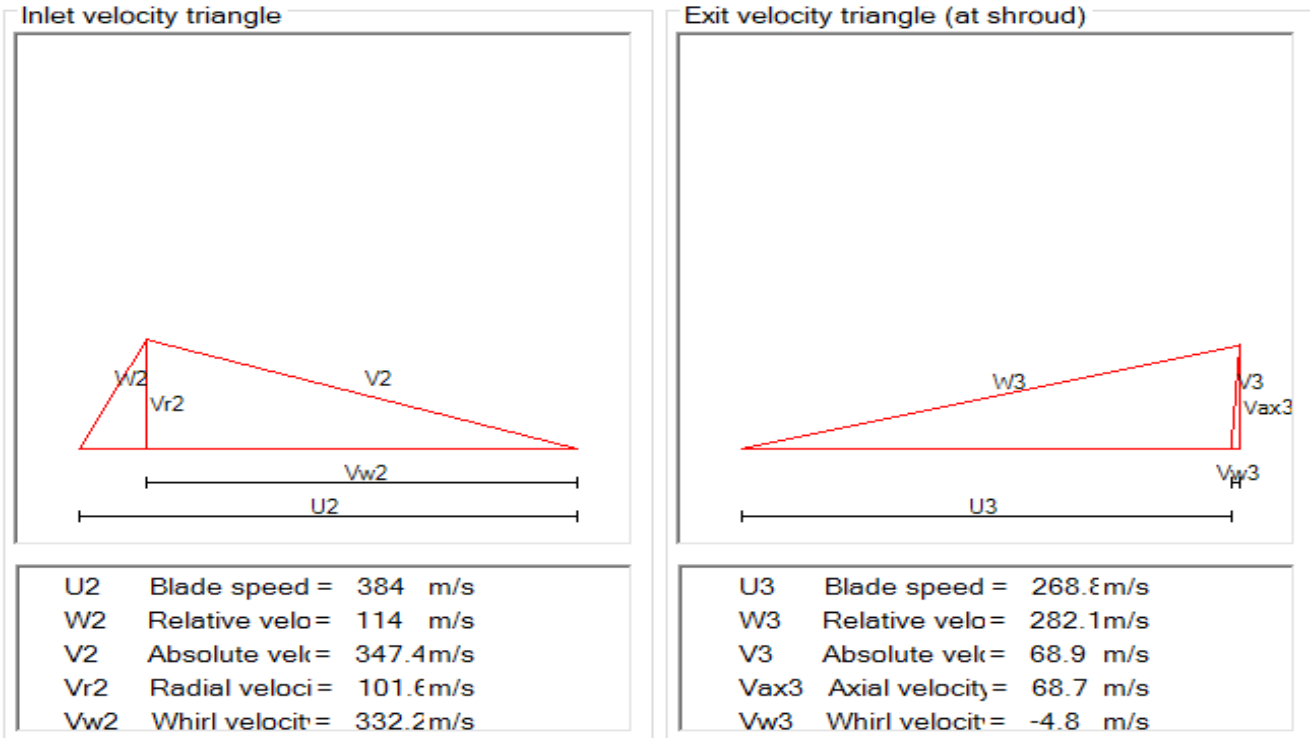

Figure 6. 1: Velocity triangle with 3D impeller

BladeGen was used to iteratively improve the flow angles by clicking and dragging the theta and beta curves. The spanwise distribution should be set to radial if it is not. The spacing of the blades at the outlet was initially too narrow due to design constraints however some spacing was desired. The realtive angle should be close to zero at the inlet so the graph was made to start at 0°. The relative flow angle was initially -80° and this was chagned to -50° to improve the spacing between the

blades. This is hown in Fig. (6.2).

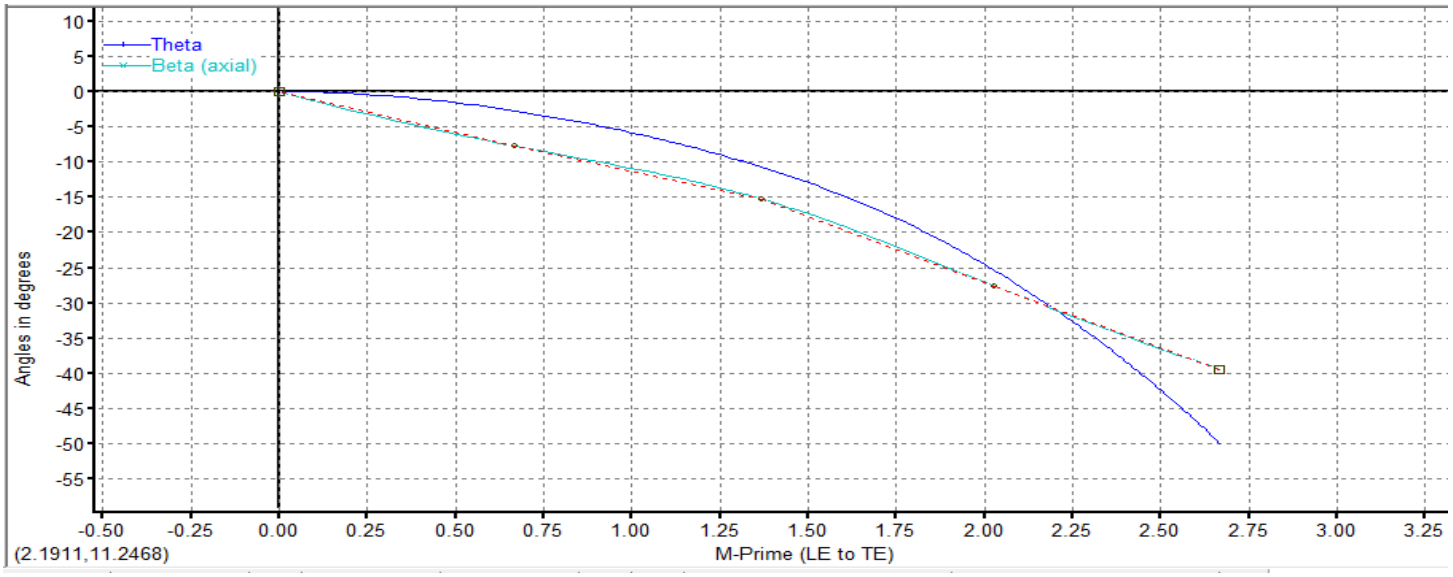

Figure 6. 2: Theta and Beta angle

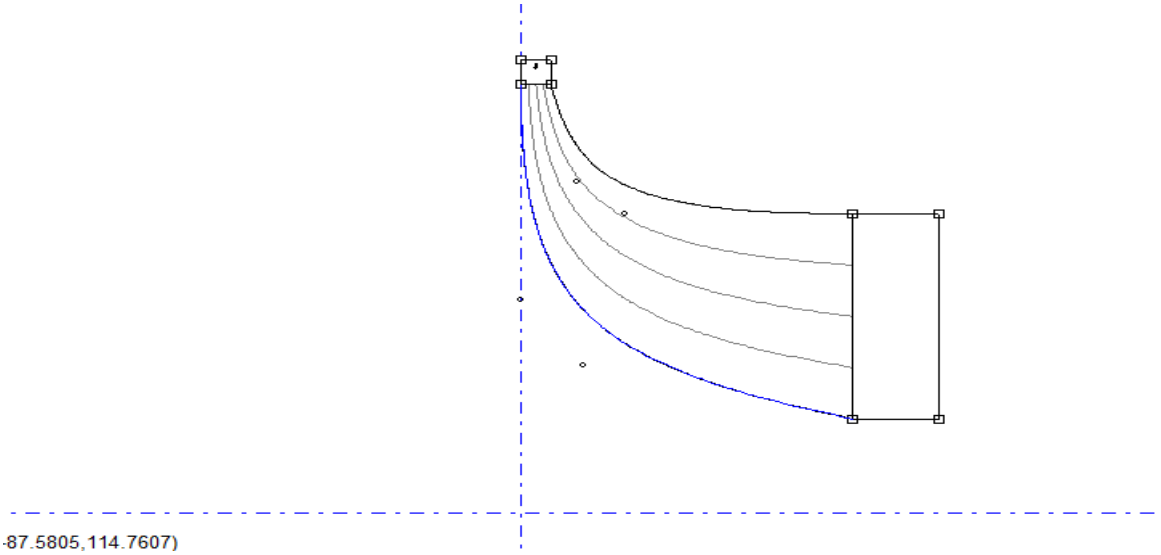

Figure 6. 3: Final Meridional profile for 100% natural gas design

At exit, a mass flow rate is still needed thus kinetic energy cannot be zero at that point. However, the absolute velocity at the exit, V3, must be minimized as much as possible otherwise that a high energy flow would increase the losses. This is the justification for using total to static efficiency as opposed to total to-total, which does not factorize the kinetic energy at the exit.

6.3 Gas blend cases

Through the utilization of the chemical properties of both natural gas and hydrogen, mass fractions calculations were executed in MATLAB to derive the properties of the blended cases. The percent volume of each mixture for the different cases were multiped by their respective molar masses and were added to determine the molar mas of the mixture. A line of code was included to make sure that

the summation added to unity after each iteration of blended cases. The mixture composition on a mass basis was then determined, which enabled other equivalent parameters to be computed such as the specific heat at constant pressure, gas constant and density. The results are summarized in Tables 6.6 and 6.7 below.

Table 6. 6: Gas properties of interest

Gas	Formula	Density kg/m^3	Cp/KJ/KgK	Cv KJ/KgK	k	R KJ/kgK	Molar Mass M kg/kmol
Hydrogen	H2	0.0838	14.301	10.183	1.405	4.124	2.016
Methane	CH4	0.668	2.254	1.7354	1.299	0.5182	16.043

Table 6. 7: Gas blend mass fraction

Natural Gas Volume	Hydrogen Volume	sum	XnG	XH	Sum	Cp_mixture	R_mixtutre, KJ/kgK	Density, kg/m^3
1	0	1	1	0	1	2.2540	0.5182	0.6680
0.95	0.05	1	0.9934	0.0066	1	2.3329	0.5419	0.6642
0.9	0.1	1	0.9862	0.0138	1	2.4197	0.5679	0.6600
0.85	0.15	1	0.9783	0.0217	1	2.5152	0.5964	0.6553

7.Numerical Analysis

7.1 Grid Generation and Mesh

TurboGrid was used due to its capability to provide high quality mesh for complex blade geometries. The impeller's geometry was transferred from BladeGen to TurboGrid. From the single periodic section, a set of geometric regions are created automatically, namely the inlet, passage, and outlet. The Automated Topology and Meshing (ATM) option was enabled to robustly create a mesh such that modification of the mesh control points would be avoided. The topology affects how the mesh is made and has a direct influence on the mesh quality. The topology set object was unsuspended to automatically create the full 3D hexahedral mesh. The user can, however, control the number of elements and nodes. Increase size factor: total elements increase and the first layer thickness decreases

An important flow phenomenon to capture is the boundary layer, which varies in thickness, δ of the order 1mm, around the blade profile. The boundary layer arises due to viscous effects which result in momentum losses, affecting the efficiency of the turbine blades. The boundary layer has several properties that were controlled using the Boundary layer refinement control and selecting a suitable method from the options. The near wall element size speciation allows the user to control the spacing distance between the wall e.g. a blade and the first layer of nodes from the wall. The y^+method was

utilized where a target y^+ is used to set the near wall spacing Δy. This target value is then specified in the passage and hub/shroud tip passages. The Reynolds number that needs to be specified is Re_L and the characteristic length is the chord of blade. This parameter is hard to predict however a good approximation coupled with the correct turbulence models allows the boundary layer to be resolved. Based on Eqn. (19) and the data from Table 6.3, a Re_L value of 751819 was calculated.

$$\Delta y = L * \Delta y^+ \sqrt{80}\, Re_x^{\frac{1}{14}} \frac{1}{Re_L} \quad (19)$$

Furthermore, a Grid Study was carried out whereby several meshes were experimented with until a suitable one was found. The correct mesh provided a satisfactory efficiency level after the solution converged. The different meshes and efficiency levels are summarized in Table 7. Fig. 7.1 and 7.2 show the final mesh of the blade geometry designed based on 100% natural gas.

Table 7. 1: Grid Study for a single case: 100% Natural Gas

Grid Study	Number of elements	Number of nodes	Efficiency
1	193152	212058	20%
2	265384	294480	95.60%
3	307495	331410	88%

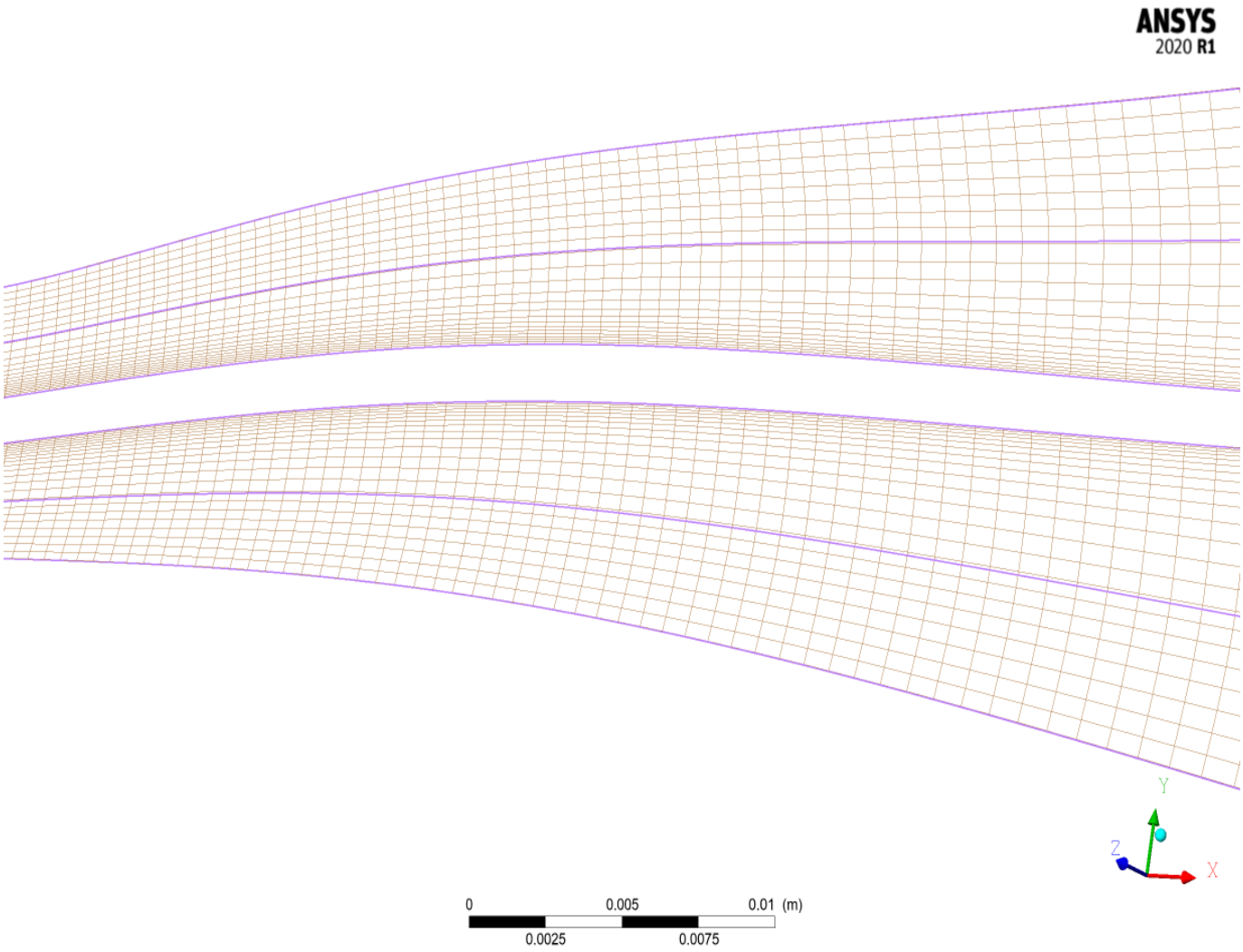

Figure 7. 1: 3D mesh of hub, revealing finer meshes near the wall

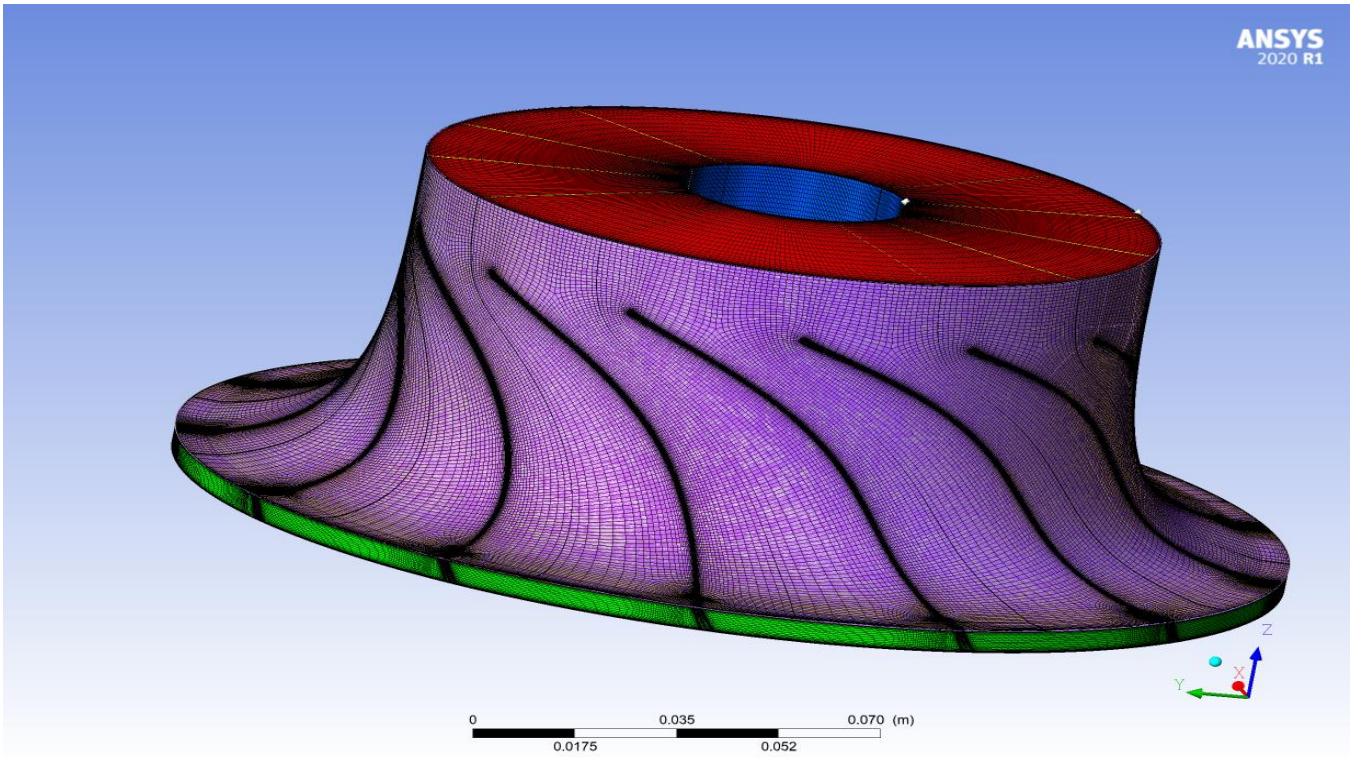

Figure 7.2: Mesh of complete geometry

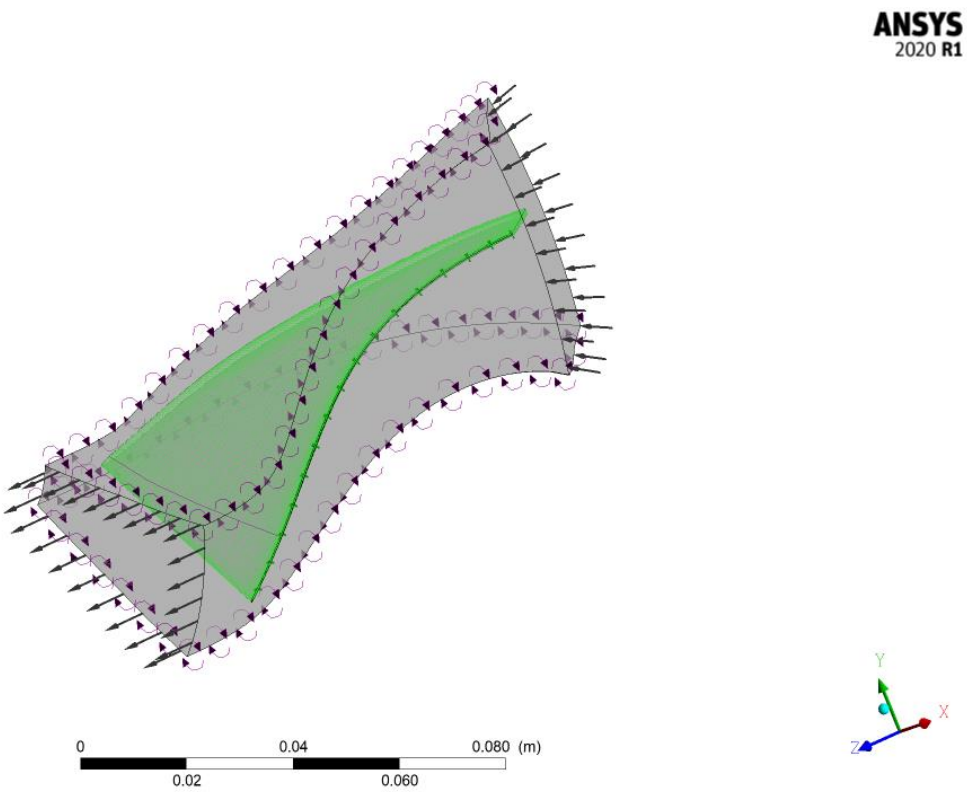

Figure 7.3: Computational Domain around Blade

7.2 CFD Analysis

Ansys CFX was used to simulate the fluid behavior in the turbine. The fluid properties from tables x-1 and x-2 where coded into Ansys CFX-pre. The gases were created and then the four different cases were constructed out of them. Fluid flow problems are governed by the nonlinear Navier Stokes equations, which needs to be solved analytically. Restrictive conditions imposed allows CFD solutions to be calculated iteratively and there are various criteria for assessing CFD convergence such as residual values. For each control volume, the local imbalance of a conserved variable is measured as residuals. The residuals can never be zero however, the lower the values, the greater the numerical accuracy of the solution. From the literature, a reasonable maximum residual level will be $\leq$ 5.0E-4, with values $\leq$4.0E-4 being considered as loosely converged (Ansys user guide,2013). A residual target of 1E-8 and a maximum iteration of 1000 was defined at this stage. The graphical user interface that was used to monitor various information about the CFD calculations and emerging solutions was CFX solver manager.

7.2.1 Results for Study one with discussion

The study of the turbine performance can be broadly divided into two parts: This first part examines how different gas blends affect the performance parameters of the turbine design based on 100% natural gas (refer to section 6.1). In the second part of the study, the performance of separate turbine geometries based on the identified gas blends are analyzed and compared with the initial design from part one.

The final convergence mass and momentum residual values for the natural gas turbine design fell within acceptable limits as shown in Fig. (7.4). A near straight line of the total-to-static efficiency is an indication convergence and once this was identified, the iteration could be stopped to save time or allowed to finish. This is shown in Fig, (7.5) and the rest of the convergence plots are placed in the appendix. The value of the efficiency at the final iteration should be used as the final value (Ansys user guide, 2016). Table 7.2 summarizes the efficiency and mass flow rate values from part one.

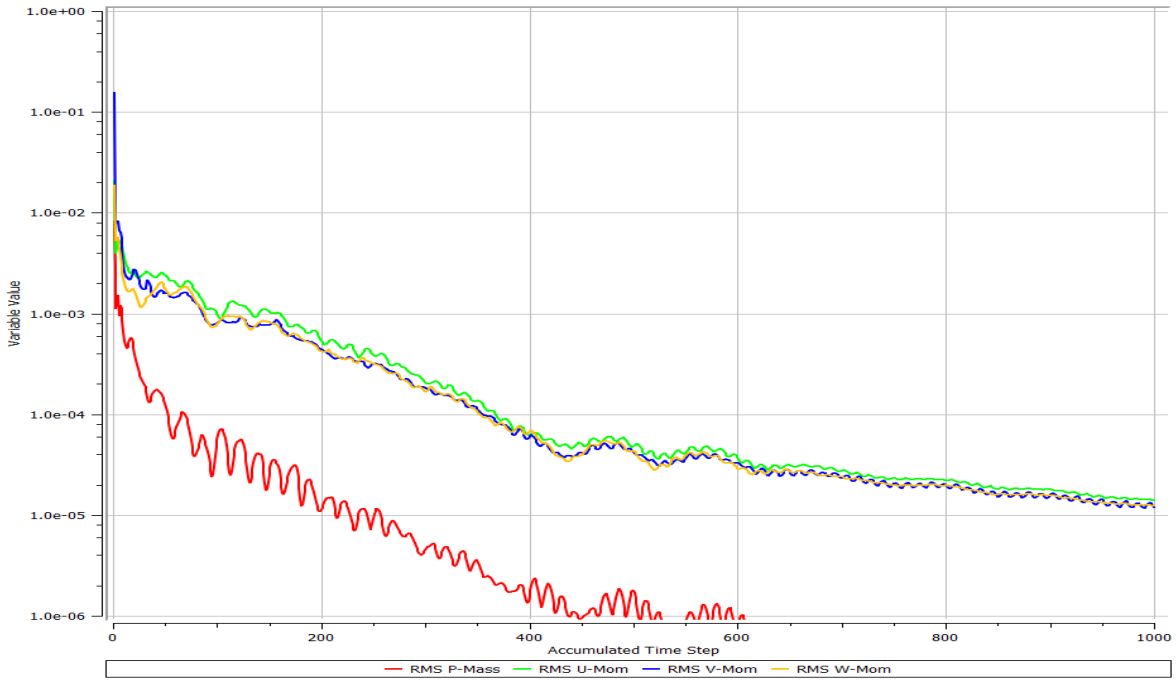

Figure 7.4: Mass and Momentum convergence for 100% Natural GasTurbine

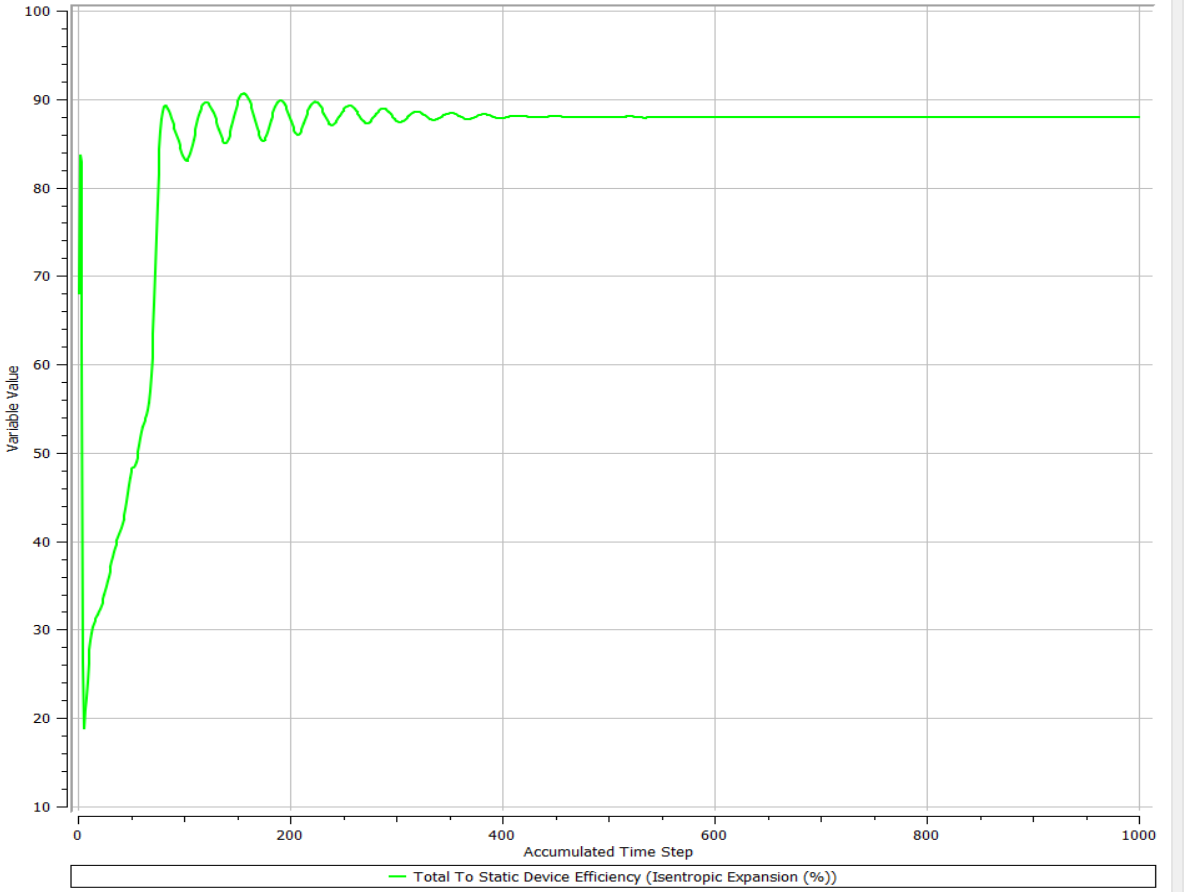

Figure 7.5: Efficiency convergence for 100% natural Gas Turbine

Table 7. 2: Summary table for study one

Cases	1	2	3	4
Vista RTD efficiency (1D). %	81.8	81.8	81.8	81.8
CFD efficiency (3D). %	88.0	78.2	71.6	70.6
% Difference of 1D vs 3D	7.6	4.4	12.5	13.7
% Difference comparison with case 1	0	11.1	18.6	19.8
Vista RTD $\dot{m}\ kg/s$	11.1	11.1	11.1	11.1
CFD $\dot{m}\ kg/s$	8.5	8.3	8.1	7.9
% Difference of 1D vs 3D	24.1	25.2	27.6	28.8
% Difference comparison with case 1	0	1.5	4.6	6.2

From Table 7.2 and from the efficiency convergence plots for study one, it is evident that the turbine would not operate at its highest level of efficiency of 88.0% at off-design conditions. The efficiency of 88% is high and corresponds to an optimum specific speed value of 0.6, which represents a 25% increase in the 1D predicted value of 0.48. This is understandable as the turbine geometric design was based on a turbine that would work with 100% natural gas The isentropic efficiency of 88% means that the turbine created is 10% more efficient than the turbine currently operating at the GRS in Velké Němčice, Czech Republic, which is also based on 100% natural gas. As the blends were added, a decrease in the efficiency of the turbine could be observed. The lowest percent difference between the efficiency values of the blends when compared to case one, was for case 2, which was a blend of 95% methane to 5% hydrogen by volume. On the other hand, the lowest efficiency was attributed to the case 4, the blend with 85% methane and 15% hydrogen.

The mass flow rate values of the different cases from the CFD results were lower than the value specified in Vista RTD, with the lowest percentage difference being attributed to the working fluid of 100% natural gas. It can also be noticed that the CFD mass flow rate values were closer to each other than the efficiency values.

For a suitable recommendation to be made, new geometries would have to be created based on the blends discussed to identify which one provides the highest efficiency.

7.2.2: Results for study two with discussion

Table 7. 3: Summary table for study two

Cases	1	2	3	4
Vista RTD efficiency (1D) %	81.8	80.9	81.4	81.5
CFD efficiency (3D) %	88.0	81.1	74.5	73.9
% Difference of 1D vs 3D	7.6	0.2	8.5	9.3
% Difference comparison with case 1	0	7.8	15.3	16.0
Vista RTD $\dot{m}\ kg/s$	11.1	11.1	11.1	11.1
CFD $\dot{m}\ kg/s$	8.5	8.7	8.8	9.8
% Difference of 1D vs 3D	24.1	21.7	20.6	12.4
% Difference comparison with case 1	0	3.1	4.6	15.4

A difference that is immediately apparent is study two compared to study one is the increase in efficiency for the gas blends – cases 2 to 4 – which is expected as the turbine geometries are optimized for each blend. The corresponding mass flow rate values also increase for a similar reason. Case 2 had the lowest percentage difference between the ID and 3D efficiency values. The CFD efficiency of 81.8% is also much closer to the 80% efficient turbine operating in Czech Republic, the only difference is that is that the turbine created operates with 5% hydrogen for the same boundary conditions as the turbine operating at the GRS station in Czech Republic, which uses 100% natural gas. This result is interesting because it means that the carbon footprint of the GRS can be decreased over several years of operation using a turbine with a higher efficiency. Furthermore, the CFD calculated mass flow rate of 8.7kg/s for case 2 is a 2.5% increase from the 100% natural gas design of 8.5kg/s. However, the lowest percentage difference between the 1D and 3D mass flow rate values was observed for the blended case of 85% methane and 15% hydrogen gas. This turbine is 8.8% less efficient than case two. The blend case of 90% methane and 10% hydrogen gas (case 3) seems to be a compromise between case 2 and 4. It can be observed that designing turbines that are based on greater proportions of hydrogen generally has a negative impact on the isentropic efficiency. However, they may be more suitable for GRS with relatively lower isentropic efficiencies.

Different countries impose different limits on the content of hydrogen in a natural gas pipeline system, which is driven by technical conditions for a given pipeline. Hydrogen content in natural gas deteriorates the energy content and has an adverse effect on the calorific value of natural gas, which explains the decrease in efficiency values for the blended cases. Some European countries have imposed a limit of 0.1 to 12% of hydrogen by volume (Kuczynski et al.,2019). Since the location of the case study is in Europe and case 2 or 3 fall within the allowable limits, it means that either the turbine design based on 5% or 10% hydrogen by volume can be recommended for this GRS.

The main benefits of adding hydrogen into the natural gas pipeline is reducing natural gas pressure drop when its being transported, which can also be happen over longer distances since no additional compressor stations will be needed.

8.Final Design output

The recommended turbine design for the GRS in Czech Republic is the one based on 95% methane and 5% hydrogen. This is because it provides decarbonization benefits whilst maintaining a high efficiency of 81.8%. The geometry of the final design can be seen in Fig. (8.1). For off-design conditions, the arrangement in Fig (8.2) can be considered.

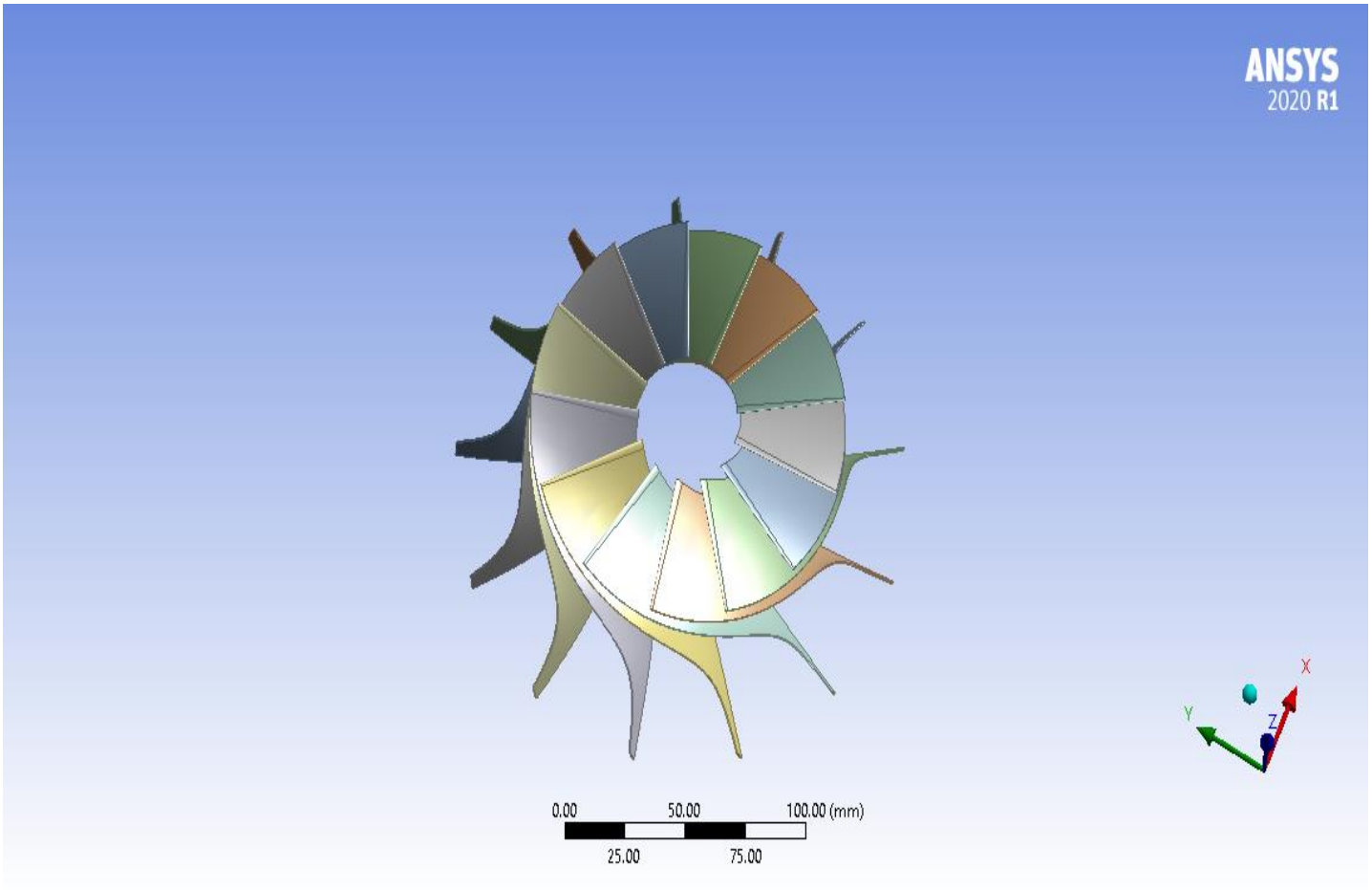

Figure 8. 1: Geometry of final design showing all 13 blades for the 95% methane and 5% hydrogen gas blend, obtained from DesignModeler.

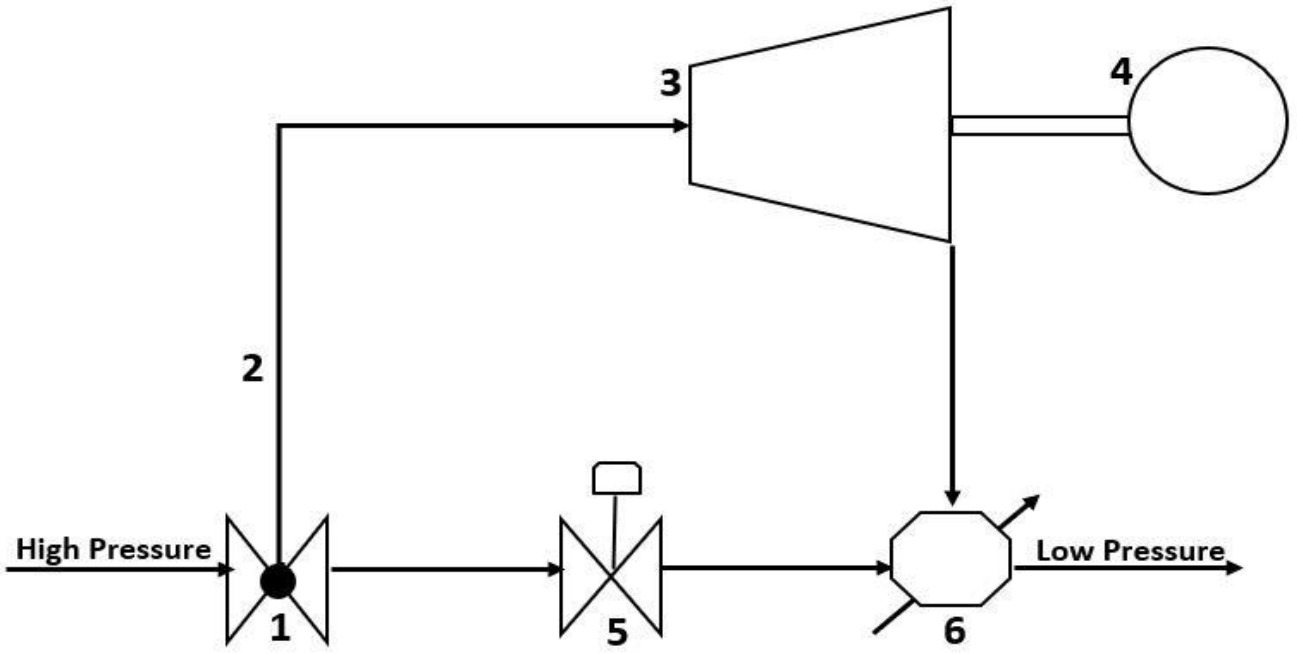

Figure 8. 1: GRS station layout, showing parallel arrangement of turbine (4) and conventional pressure valve (5) Key: 1 - Shut down valve, 2 – Flow path to turbine, 3 – Turbine, 4 – Electricity generator with shaft, 5 – conventional pressure regulator valve, 6 – post heating.

9.Conclusions

To conclude, this project explored the effect of adding hydrogen into an existing natural gas turbine from a performance perspective. It was discovered that within limits, a blended gas radial expander can provide some beneficial effects in the form of a greener GRS without decreasing the efficiency of the 100% natural gas turbomachine design.

TBC

10.Limitations & Recommendations

.
Installing a turbo-expander is a huge investment and there are several ideas to keep in mind. Going for post heating option saves money and can provide electricity to some 50 houses. Wherever it is possible, efficiency should be improved, which is becoming more important due to imperatives and legal requirements in some countries. That said, fundings in deploying technology on wide scale is difficult. The electrical generator close to pipeline is a safety concern. System should be fully sealed such that In case of any spark, there are no explosions.

The project was affected by an issue associated with the Ansys software. The CFX-post results that would enable boundary conditions to be confirmed was unable to open despite several attempts and with the consultation of senior users of the software, including the supervisor, Dr. Jafar Al-Zaili. The issue was also raised to IT who could not resolve the issue.

11.Bibliography

TBC

12. Appendix

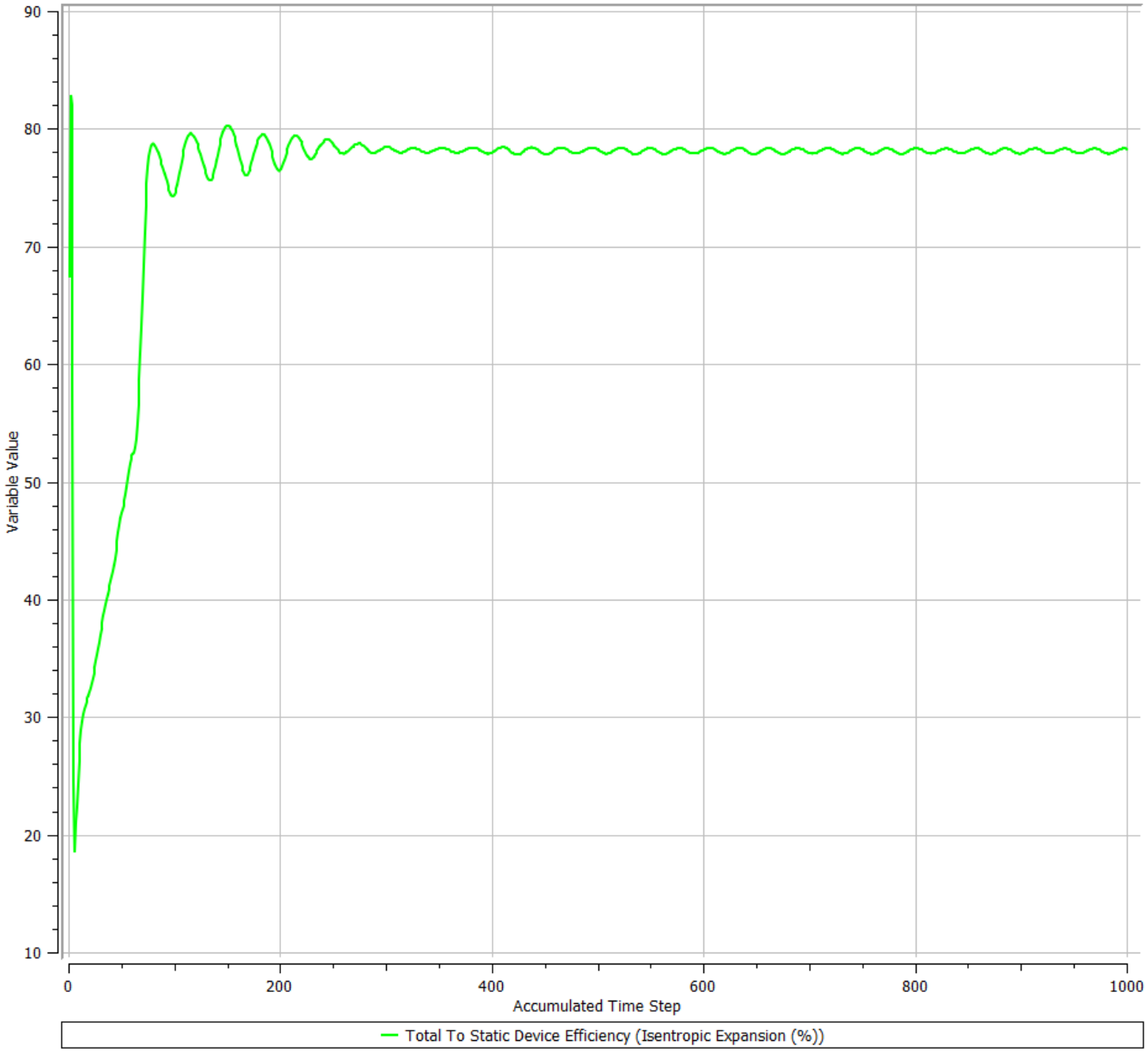

95% using natural gas blends

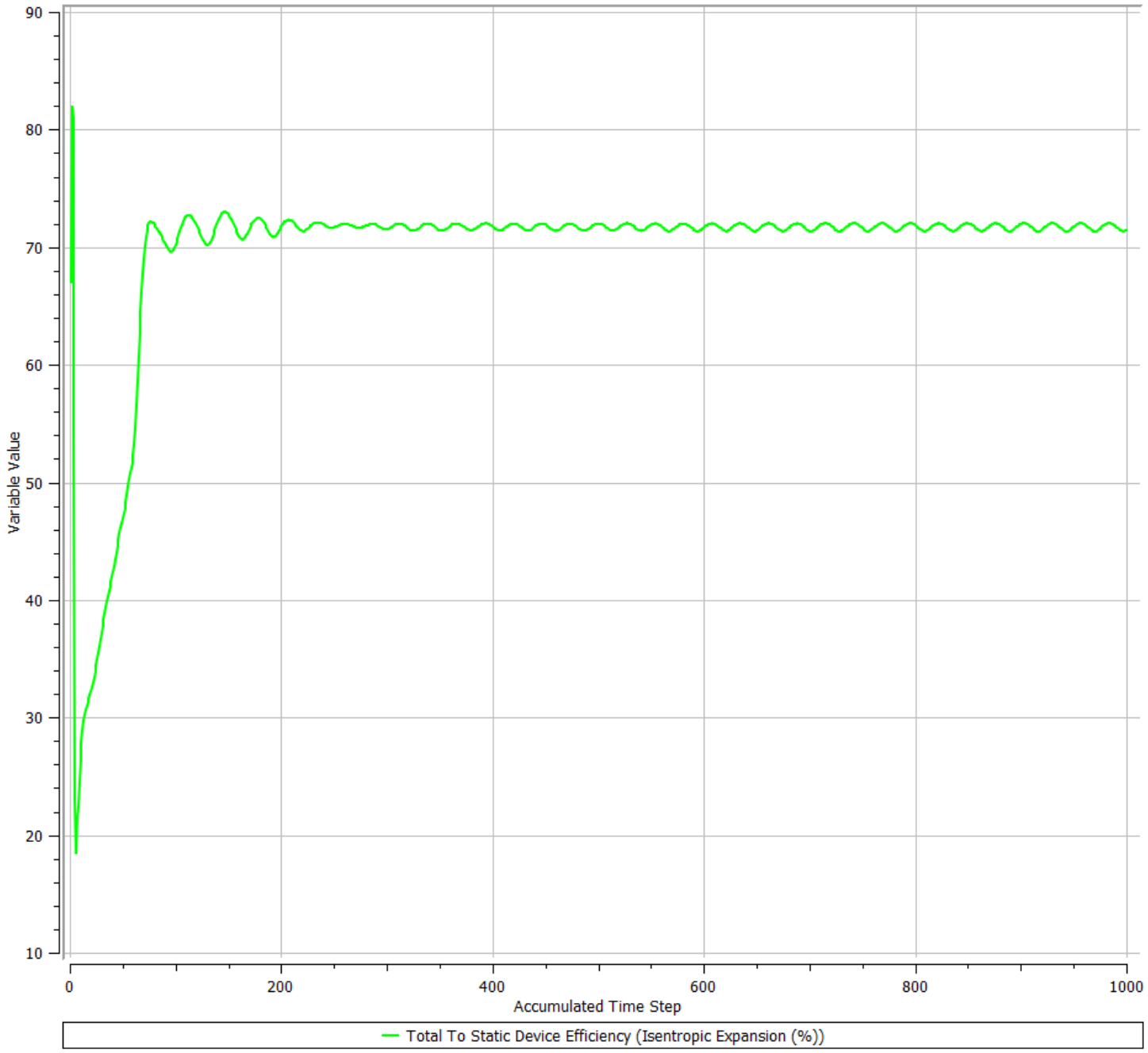
90
80
70
60
50
40
30
20
10
Variable Value
0
200
400
600
800
1000
Accumulated Time Step
Total To Static Device Efficiency (Isentropic Expansion (%))

90%

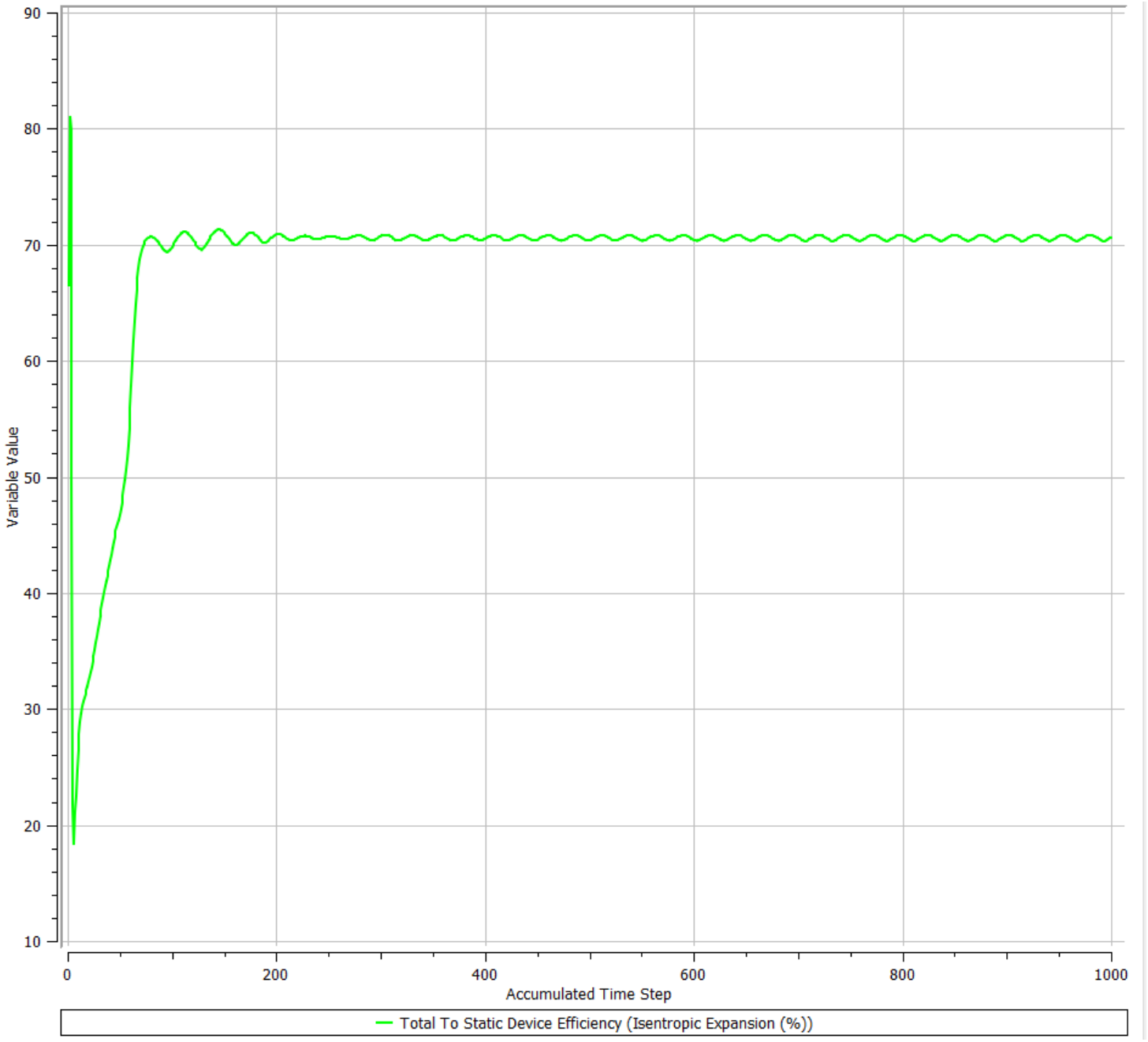

85% based on methane design

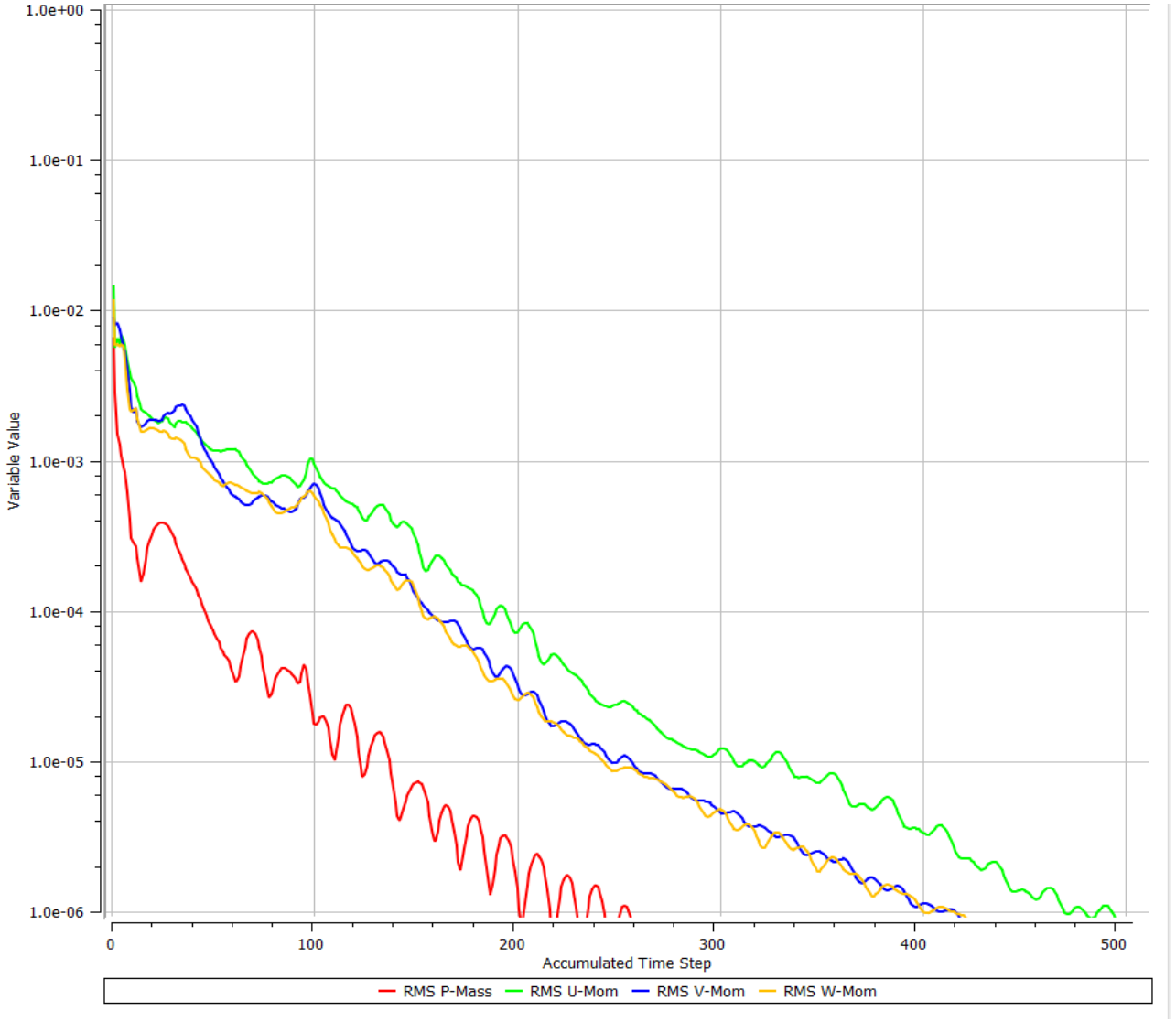
1.0e+00
1.0e-01
1.0e-02
1.0e-03
1.0e-04
1.0e-05
1.0e-06
Variable Value
0
100
200
300
400
500
Accumulated Time Step
RMS P-Mass
RMS U-Mom
RMS V-Mom
RMS W-Mom

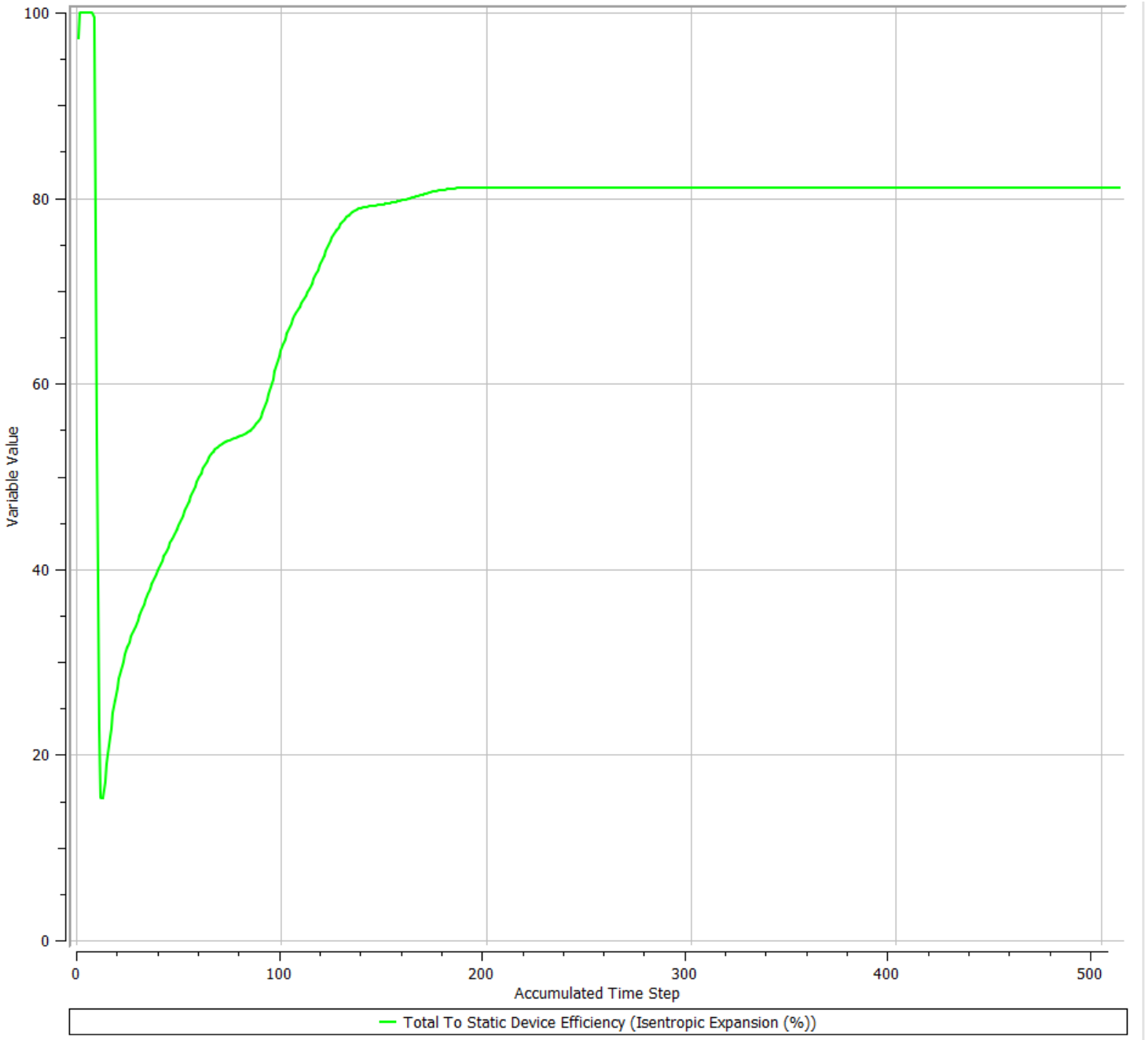
100
80
60
40
20
0
Variable Value
0
100
200
300
400
500
Accumulated Time Step
Total To Static Device Efficiency (Isentropic Expansion (%))

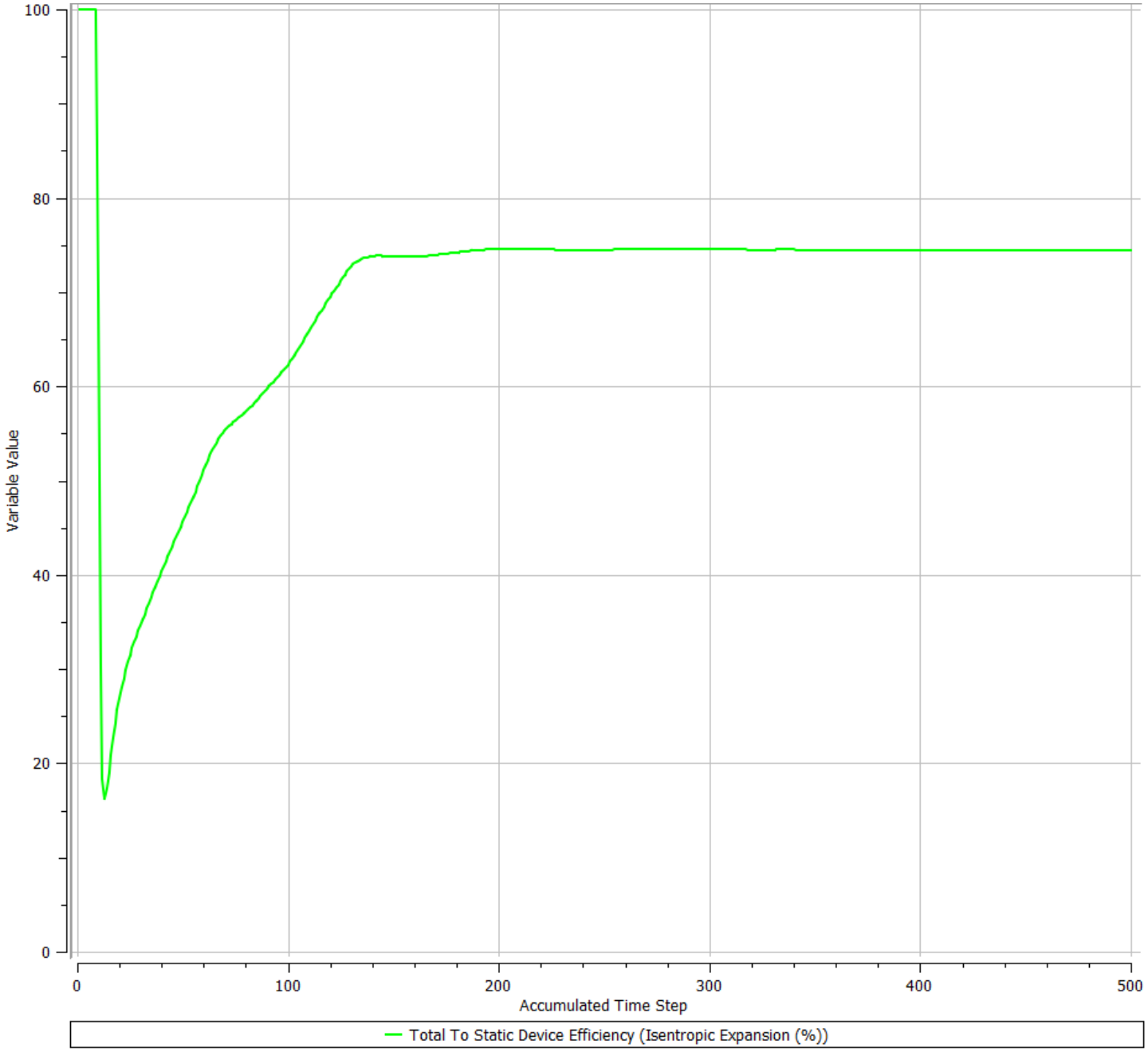
100
80
60
40
20
0
Variable Value
0
100
200
300
400
500
Accumulated Time Step
Total To Static Device Efficiency (Isentropic Expansion (%))

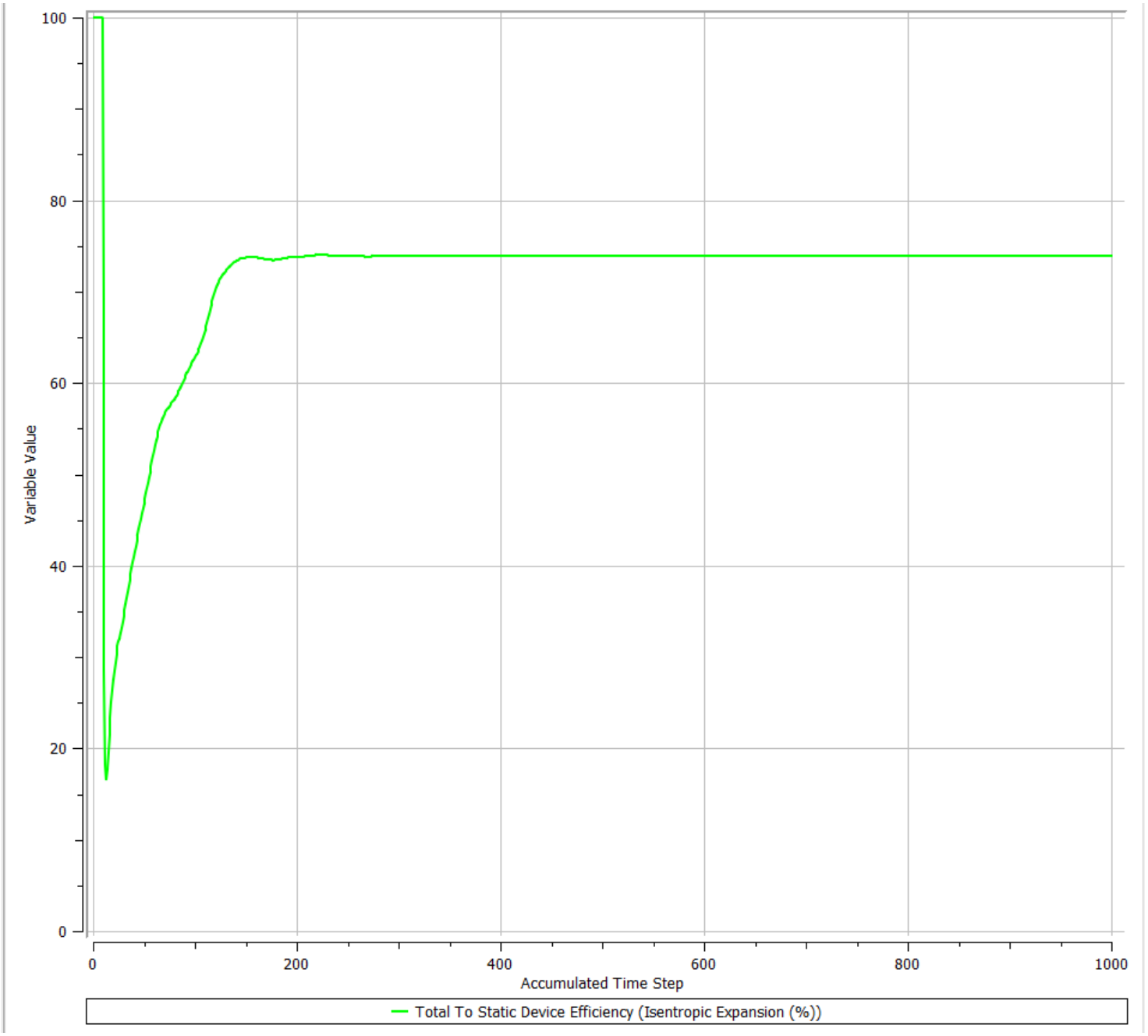

12.1 Appendix A

```
clear
close all
clc
%% Which requires less energy Pre-heating or Post heating?
% Initialisation
eta = 0.8; %isentropic efficiency
eta2 = 0.97; % gearbox or mechanical
eta3 = 0.95; % efficeicy of generator
m_dot = 11.13; %kg/s
T2 = 290;  %k and equal to T_out lower due to losses in pipes
R_methane = 0.5182; %KJ/Kg.K
M_methane = 16.043; %Molecular weight of methane gas in Kg/Kmol
%defining constants for Methane valid for T (K): 273<T<1500
a = 19.89;
b = 5.024e-2;
c = 1.269e-5;
d = -11.01e-9;
%Cp Polynomial (Temperature)Function: Max % error:1.33 Avg. = 0.57
c_p1 = a+b*T2+c*T2^2+d*T2^3; %KJ/kmolK
c_p1_corrected = c_p1/M_methane; %KJ/kgK
%Boundary conditions of Turbine
p1 = 5.5e6;
p2 = 1.8e6;
c_v1 = c_p1_corrected - R_methane;
k = c_p1_corrected/c_v1;
w = (p2/p1)^((k-1)/k);
T1 = T2/(eta*(w-1+(1/eta))) % Preheat temp where w is just a constant
%Heat Calculation
%Cp Polynomial (Temperature)Function: Max % error:1.33 Avg. = 0.57
T_avg = (T1+T2)/2;
c_p_avg = a+b*T_avg+c*T_avg^2+d*T_avg^3; %KJ/kmolK
c_p_avg_corrected = c_p_avg/M_methane;
Qin_pre = m_dot*c_p_avg_corrected*(T1-300) %kw t2 should be Tin
% which is 300k! (T1 -Tin) T1 is 355.9K
```

```
%% For post heating
T1_new = 290; %K %tout
%Cp Polynomial (Temperature)Function: Max % error:1.33 Avg. = 0.57
c_p2 = a+b*T1_new+c*T1_new^2+d*T1_new^3;%KJ/kmolK
c_p2_corrected = c_p2/M_methane; %KJ/kgK
%Boundary conditions of Turbine
p1 = 5.5e6;
p2 = 1.8e6;
c_v2 = c_p2_corrected - R_methane;
k_new = c_p2_corrected/c_v2;
w2 = (p2/p1)^((k_new-1)/k_new);
T2_new = T1_new*eta*(w2-1+(1/eta)) % T2
T_avg2 = (T1_new+T2_new)/2;
c_p2_avg = a+b*T_avg2+c*T_avg2^2+d*T_avg2^3; %KJ/kmolK
c_p2_avg_corrected = c_p2_avg/M_methane;
Qin_post = m_dot*c_p2_avg_corrected*(T1_new-T2_new)%kw should be (Tout -T2)
% Tout is 290K and T2 is 236.3K

%%  Turbine power output
Wt1 = m_dot*c_p_avg_corrected*(T1-T2) %Turbine power, where t1 is 355.9k
%and t2 is 290K
Wt2 = m_dot*c_p2_avg_corrected*(300-T2_new)% t1 is tout which is 300K
% and T2 is 290 and t2_new is 236.3k (Tout - T2)

%% Net Electric power total electric - heat required
Wnet_preheat = eta2*Wt1*eta3 - Qin_pre
Wnet_postheat= eta2*Wt2*eta3 - Qin_post

%% Specific Power
wnet_dot_preheat = Wnet_preheat/m_dot
wnet_dot_postheat = Wnet_postheat/m_dot
```

```
clear
close all
clc
%% Mass Fraction Calculations
%Initialisation
R =8.3143; %kj/kgmole*K
M_m =16.043; %kg/kmol
M_h =2.016; %kg/kmol
K_m =1.299;
K_h =1.405;
rho_m =0.668;
rho_h =0.08375;
%these are the mole fractions given as volumes
Vol_m = 0.85;
Vol_h = 0.15;
Sum_1 = Vol_m+Vol_h
%S1.Equivalent molecular mass of mixture
M_eqv = M_m*Vol_m +M_h*Vol_h;
%S2.Mixture composition on Mass basis
X_m = Vol_m*(M_m/M_eqv)
X_h = Vol_h*(M_h/M_eqv)
Sum_2 = X_h+X_m
%S3.Determine R_mixture
R_eqv = R/M_eqv
```

```
  %S2.Mixture composition on Mass basis
  X_m = Vol_m*(M_m/M_eqv)
  X_h = Vol_h*(M_h/M_eqv)
  Sum_2 = X_h+X_m
  %S3.Determine R_mixture
  R_eqv = R/M_eqv
  R_eqv2 = X_m*0.5182 +X_h*4.124
  %S4.Determine cp_mixture
  Cp_eqv = X_m*2.2537 +X_h*14.307
  %S5.Determine rho_mixture
  rho_eqv = X_m*rho_m +X_h*rho_h
```